Apolipoproteins E and CIII interact to regulate HDL metabolism and coronary heart disease risk

Allyson M. Morton,[1] Manja Koch,[1] Carlos O. Mendivil,[1,2,3] Jeremy D. Furtado,[1] Anne Tjønneland,[4] Kim Overvad,[5,6] Liyun Wang,[1] Majken K. Jensen,[1,7] and Frank M. Sacks[1,7,8]

[1]Department of Nutrition, Harvard T.H. Chan School of Public Health, Boston, Massachusetts, USA. [2]Department of Medicine, Universidad de los Andes, Bogotá, Colombia. [3]Section of Endocrinology, Department of Internal Medicine, Fundación Santa Fe de Bogotá, Bogotá, Colombia. [4]Danish Cancer Society Research Center, Copenhagen, Denmark. [5]Department of Cardiology, Aalborg University Hospital, Aalborg, Denmark. [6]Section for Epidemiology, Department of Public Health, Aarhus University, Aarhus, Denmark. [7]Channing Division of Network Medicine, Department of Medicine, Brigham and Women's Hospital, Harvard Medical School, Boston, Massachusetts, USA. [8]Department of Genetics and Complex Diseases, Harvard T.H. Chan School of Public Health, Boston, Massachusetts, USA.

BACKGROUND. Subspecies of HDL contain apolipoprotein E (apoE) and/or apoCIII. Both proteins have properties that could affect HDL metabolism. The relation between HDL metabolism and risk of coronary heart disease (CHD) is not well understood.

METHODS. Eighteen participants were given a bolus infusion of [D3]L-leucine to label endogenous proteins on HDL. HDL was separated into subspecies containing apoE and/or apoCIII and then into 4 sizes. Metabolic rates for apoA-I in HDL subspecies and sizes were determined by interactive modeling. The concentrations of apoE in HDL that contain or lack apoCIII were measured in a prospective study in Denmark including 1,949 incident CHD cases during 9 years.

RESULTS. HDL containing apoE but not apoCIII is disproportionately secreted into the circulation, actively expands while circulating, and is quickly cleared. These are key metabolic steps in reverse cholesterol transport, which may protect against atherosclerosis. ApoCIII on HDL strongly attenuates these metabolic actions of HDL apoE. In the epidemiological study, the relation between HDL apoE concentration and CHD significantly differed depending on whether apoCIII was present. HDL apoE was associated significantly with lower risk of CHD only in the HDL subspecies lacking apoCIII.

CONCLUSIONS. ApoE and apoCIII on HDL interact to affect metabolism and CHD. ApoE promotes metabolic steps in reverse cholesterol transport and is associated with lower risk of CHD. ApoCIII, when coexisting with apoE on HDL, abolishes these benefits. Therefore, differences in metabolism of HDL subspecies pertaining to reverse cholesterol transport are reflected in differences in association with CHD.

TRIAL REGISTRATION. Clinicaltrials.gov NCT01399632.

FUNDING. This work was supported by NIH grant R01HL095964 to FMS and by a grant to the Harvard Clinical and Translational Science Center (8UL1TR0001750) from the National Center for Advancing Translational Science.

Introduction

Despite advances in research and clinical care, cardiovascular disease (CVD) remains the leading cause of mortality in the US, accounting for about 1 in 3 deaths each year (1). Epidemiological studies unequivocally demonstrate a strong inverse relationship between HDL, measured by its cholesterol content (HDL-C) or by its primary protein apolipoprotein (apo) A-I, and risk of CVD (2, 3). HDL is thought to exert its cardioprotective effects, in part, by removing excess cholesterol from cells that are present in atherosclerosis and transporting it to the liver for excretion, a process known as reverse cholesterol

Authorship note: AMM and MK contributed equally to this work.

Conflict of interest: FMS was a consultant to Pfizer on drug development and was an expert witness on cases involving Aegerion and Pfizer. FMS, MKJ, and JDF are inventors on patents awarded to Harvard University pertaining to HDL: US 8,846,321 B2 and US 9,494,606 B2.

Submitted: October 12, 2017
Accepted: January 17, 2018
Published: February 22, 2018

Reference information:
JCI Insight. 2018;3(4):e98045.
https://doi.org/10.1172/jci.insight.98045.

transport. However, the failure of large-scale studies that raised HDL-C levels without reducing risk of coronary heart disease (CHD) (4–7) has stimulated research on the protein cargo on HDL and its ability to mediate HDL function.

It is becoming increasingly recognized that HDL is a heterogeneous particle system that carries a vast array of proteins with heterogeneous biological functions (8) involved in lipid metabolism, reverse cholesterol transport, and other conditions. These resident proteins likely form distinct subpopulations, or subspecies, of HDL that may capture its functional relationships with cardiometabolic disease and relation to CHD more so than total HDL-C concentrations (9). However, little is known about the effect of these subspecies on HDL metabolism and CHD in humans.

ApoE affects the metabolism of apoB-containing lipoproteins, offering insight as to how it might affect HDL metabolism in humans. ApoE binds to LDL-receptor (LDL-R) (10), LDL-R related protein (LRP) (11), and heparin/heparan sulfate proteoglycans (12–15). In humans, VLDL and IDL that contain apoE are cleared from the circulation much more quickly than those without apoE (16, 17). Much less is known about apoE as a component of HDL. In vitro, apoE facilitates size expansion of HDL (18–20) due to its interaction with phospholipid polar head groups on HDL particles (21), which assist in enrichment of the HDL core with cholesterol ester. In mice, apoE promotes HDL biogenesis by interacting with ABCA1 independently of apoA-I (22). ApoE can also mediate holoparticle uptake of HDL into hepatocytes and other cells (23–25). Receptor binding studies in cultured human fibroblasts showed that HDL containing apoE from patients with abetalipoproteinemia (a condition in which no apoB-containing lipoproteins are synthesized) outcompeted radiolabeled LDL in binding to LDL-R, implying that apoE can effectively mediate HDL holoparticle uptake (26). Finally, Ikewaki et al. (27) exogenously labeled apoA-I and apoE and reassociated them with autologous lipoproteins in patients with abetalipoproteinemia to assess whether apoE had an effect on apoA-I metabolism. They demonstrated that apoA-I on apoE-containing HDL was cleared from the circulation faster than apoA-I on HDL that does not contain apoE. This finding suggests that apoE may affect metabolism of native HDL in normal humans, in vivo.

ApoCIII delays clearance of apoB-containing lipoproteins, but little is known about its role in HDL metabolism. In vitro, apoCIII inhibits the binding of apoE and apoB to LDL-R and other receptors (28). In humans, VLDL and IDL that contain apoCIII are cleared more slowly from plasma than VLDL and IDL that do not contain apoCIII (29, 30). Fibrates, which are PPARα agonists, lower plasma apoCIII as one of their actions on the lipoprotein system and increase clearance not only of apoB-containing lipoproteins, but also of HDL apoA-I (31). That reduction in plasma apoCIII is correlated with increased clearance of HDL apoA-I (31). These findings offer a hypothesis that apoCIII slows HDL clearance, which could have important implications for CVD pathophysiology.

In addition to their individual roles, apoE and apoCIII act in opposition to modulate the clearance of apoB-containing lipoproteins. In fibroblasts, apoCIII inhibits the apoE-dependent uptake of VLDL by LDL-R (28, 32). Addition of apoCIII to apoE-enriched chylomicrons in rats results in a pronounced inhibition of clearance of hepatic chylomicron and triglyceride emulsions (33). In mice, overexpression of apoCIII reduces VLDL clearance, and this action is rescued by either exogenous apoE or genetic apoE overexpression (34). Similarly, coexpression of the apoE transgene in *APOC3* transgenic mice eliminates the hypertriglyceridemia caused by apoCIII (34, 35). Finally, in kinetic studies of human VLDL and IDL, apoCIII overrides the increased clearance promoted by apoE (17, 30, 36). It is unknown if apoE and apoCIII function similarly on HDL.

The clinical implications of apoE on HDL are still poorly defined, potentially due to the presence of other proteins obscuring its true effect. Among 5 proteins on HDL found to differ in control subjects and participants with coronary artery disease (CAD), apoE was discovered to be the most abundant protein in HDL isolated from atherosclerotic lesions (37), suggesting an important role of apoE in HDL in atherosclerosis pathophysiology. The few studies available examining the relation of apoE in HDL to CVD outcomes were together inconclusive (38, 39). In previous work in the Nurses' Health Study, the Health Professionals Follow-Up Study, the Multi-Ethnic Study of Atherosclerosis, and the Danish Diet, Cancer, and Health (DCH) study — 4 large prospective cohort studies — we found that the association of HDL with CHD risk was modified by the presence of apoCIII (40). HDL containing apoCIII was associated with higher risk of CHD, whereas HDL not containing apoCIII was associated with lower CHD risk.

The aims of this study were to determine if apoE and/or apoCIII has effects on human HDL metabolism and whether the effects on metabolism had clinical counterparts in CHD risk. We hypothesized that

Table 1. Characteristics of participants in the metabolic study and the case-cohort study nested in the Danish DCH study

	Metabolic study[A]		Case-cohort study[B]		
Variable	**Full set with HDL E^+, E^- measurement (*n* = 18)**	**Subset with HDL apoE and/or apoCIII measurement (*n* = 10)**	**Random subcohort (*n* = 1,750)**	**CHD (*n* = 1,946)**	***P* for difference**
Age, yrs	49 (23, 70)	49 (23, 70)	56 (51, 64)	59 (51, 65)	<0.001
Male	9 (50)	4 (40)	933 (53)	1,419 (73)	<0.001
Current smoker	NA	NA	662 (38)	1070 (55)	<0.001
Alcohol intake, g/day[C]	0	0	14 (1, 66)	14 (0.2, 69)	0.69
BMI, kg/m^2	30 (26, 36)	31 (26, 36)	26 (20, 33)	27 (21, 35)	<0.001
Hypertension[D]	3 (17%)	2 (20%)	259 (15)	498 (26)	<0.001
Diabetes[D]	0 (0)	0 (0)	31 (2)	107 (6)	<0.001
LDL-C[E], mg/dl	117 (59, 184)	106 (59, 147)	137 (87, 197)	151 (92, 210)	<0.001
HDL-C, mg/dl	45 (24, 54)	46 (24, 54)	52 (27, 90)	46 (24, 89)	<0.001
Triglycerides, mg/dl	112 (50, 271)	80 (62, 262)	81 (36, 237)	108 (43, 304)	<0.001
HDL-ApoA-I[F], mg/dl	100 (73, 147)	111 (73, 147)	136 (78, 224)	134 (74, 230)	0.04
Plasma apoCIII[G], mg/dl	8 (3.5, 13.5)	8 (3.5, 13.5)	11 (4, 23)	11 (4, 24)	0.76
Plasma apoE, mg/dl	6.0 (4.0, 9.5)	6.5 (4.0, 9.5)	NA	NA	
ApoE genotype			NA	NA	
E3/E3	9 (50)	4 (40)			
E2/E3	1 (6)	0 (0)			
E4/E3	6 (33)	4 (40)			
E2/E4	2 (11)	2 (20)			

[A]Median (range) or *n* (%). [B]Median (5th and 95th percentiles) or *n* (%). [C]*n* = 3 missing. [D]Self-reported physician diagnosis of hypertension or diabetes. [E]*n* = 95 missing in random subcohort and *n* = 984 missing in CHD cases. [F]The concentration of HDL was quantified based on apoA-I levels, the major apolipoprotein component of HDL. [G]*n* = 1 missing in random cohort.

HDL containing apoE would participate in reverse cholesterol transport, a hallmark of HDL antiatherogenic function. We considered crucial aspects of reverse cholesterol transport to be (i) evidence of size expansion followed by (ii) increased clearance rates from the circulation. We also hypothesized that HDL containing apoCIII would have an attenuated clearance rate in vivo. Clinically, we hypothesized that apoE in HDL would be inversely related to incident CHD and that apoCIII would mitigate this protective effect. We carried out these aims in a metabolic study in humans and a prospective case-cohort study nested in a large community-based sample.

Results

For the metabolic study, we enrolled 18 adults (9 male and 9 female; Table 1). Participants had low HDL-C (<45 mg/dl for males, <55 mg/dl for females) and were overweight (BMI ≥ 25 kg/m^2). The median apoA-I concentration in plasma was 100 mg/dl. Plasma concentrations of apoE and apoCIII were normal. We studied apoA-I–containing HDL subspecies containing apoE (E^+) or not containing apoE (E^-) in all 18 participants, and HDL subspecies containing apoE and/or apoCIII in a subset of 10 participants (4 male, 6 female).

ApoA-I metabolism of 4 HDL sizes. After administering a high unsaturated fat control diet for 4 weeks, we infused study participants with a bolus of trideuterated leucine (5,5,5-D3 L-leucine, D3-leucine), and we isolated and purified apoA-I from plasma collected over time (Figure 1). To compare with the metabolism of a human population we have previously studied (41), we first modeled the metabolism of plasma apoA-I in 4 sizes of HDL (Figure 2). The large- and medium-sized HDL (42), α-2 and α-3, are the major size fractions of HDL in these participants, accounting for about 75% of total apoA-I mass (Figure 2A). Discoidal prebeta HDL comprises about 10% of plasma apoA-I. We modeled the tracer enrichment curves and masses using SAAM-II, a commercially available modeling software (43). We found that the model that provided excellent fits to the data is characterized by direct secretion of all 4 sizes of HDL and size contraction from α-3 to prebeta, representing prebeta generation (Figure 2B). We called this the bare-minimum model due to its parsimony (for additional information on model development, please see the Supplemental Methods; supplemental material available online with this article; https://doi.org/10.1172/jci.insight.98045DS1).

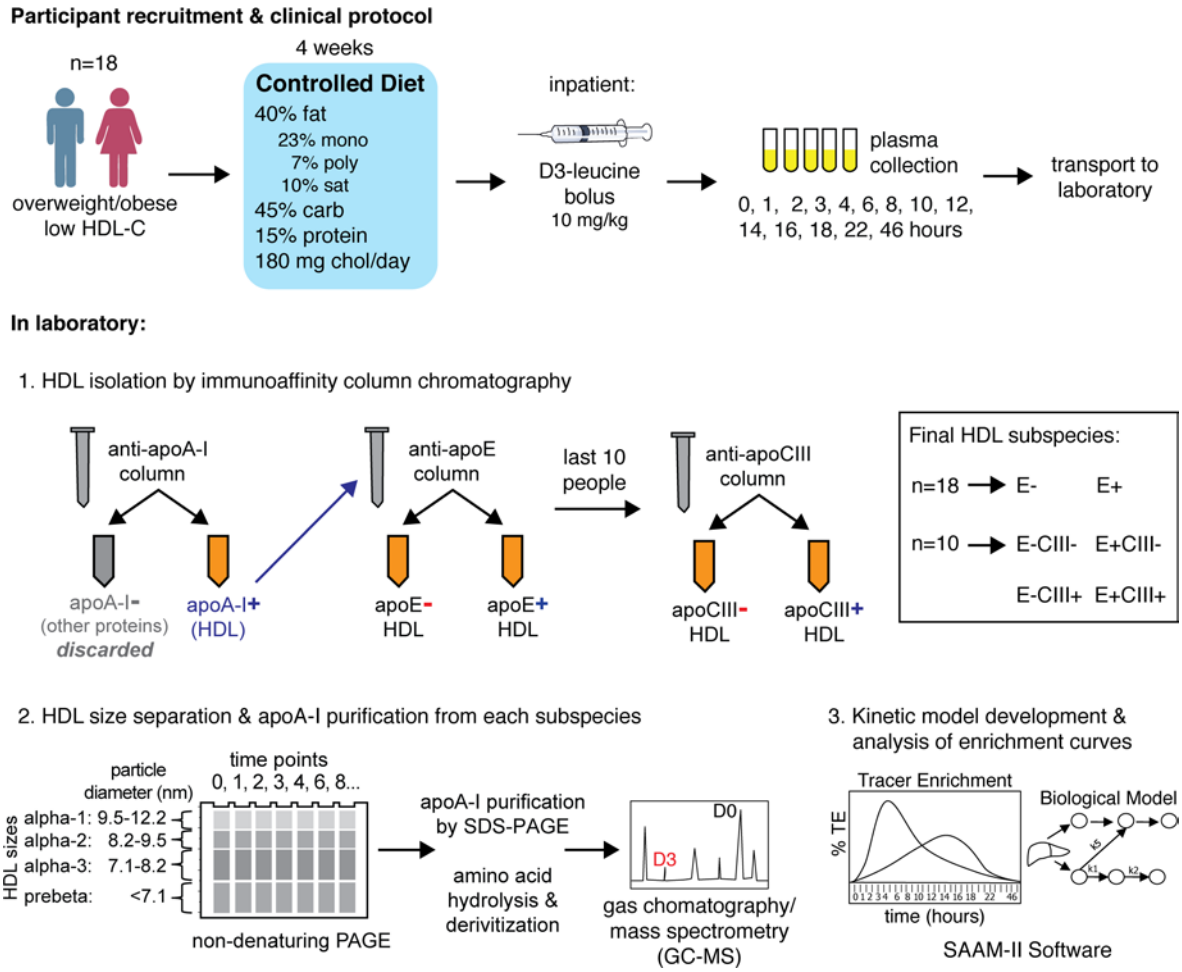

Figure 1. Overview of clinical protocol and laboratory methods.

The tracer enrichment curves (Figure 2C) and pool sizes (Figure 2D) with SAAM-II model fits are shown for the average of 18 people for 4 sizes of HDL. Fractional catabolic rates (FCRs), representing turnover of apoA-I, were about 0.4 pools/day for apoA-I on α-1, -2, and -3 HDL and 3.7 pools/day for prebeta (Figure 2E and Supplemental Table 1). These results are consistent with those in a previous report in a separate group of humans (41).

ApoA-I metabolism on HDL containing or not containing apoE. To model the tracer enrichments and pool sizes of apoA-I of the HDL subspecies, we started with the previous well-characterized bare-minimum model for plasma apoA-I across 4 HDL sizes (Figure 3A and Figure 2B). However, the apoA-I of E^+ HDL required size expansion from prebeta to α-1 and α-2 to fit the tracer enrichment curves (Figure 3B). This flux pathway was not needed to fit E^- HDL. Figure 3C shows the tracer enrichment curves and model fits of apoA-I tracer enrichments on E^- HDL and E^+ HDL. Compared with E^- HDL, the tracer enrichment curves of apoA-I in E^+ HDL had steeper slopes to and from the peak, generally indicative of faster turnover. The FCR of apoA-I on E^+ HDL was about 8, 4, and 4 times faster than that of E^- HDL for α-1, -2, and -3 respectively ($P \leq 0.001$ for all, paired 2-tailed *t* test) and not significantly different for prebeta HDL ($P = 0.13$) (Figure 3D and Supplemental Table 1). Only about 4% of apoA-I HDL contained apoE (Figure 3E). The size distributions for apoA-I in E^+ and E^- HDL were similar.

ApoA-I on HDL containing or not containing apoCIII. We also wanted to determine if there was a unique effect of apoCIII on HDL metabolism (as was seen with apoE) (Figure 4). We used the same bare-minimum model established for E^- HDL (Figure 3A, Figure 2B) to model the tracer enrichment curves for apoA-I in $CIII^-$ (Figure 4A) and $CIII^+$ (Figure 4B) HDL. The enrichment curves for both subspecies appeared similar and were both visually similar to those of plasma apoA-I and E^- HDL (Figure 2C and

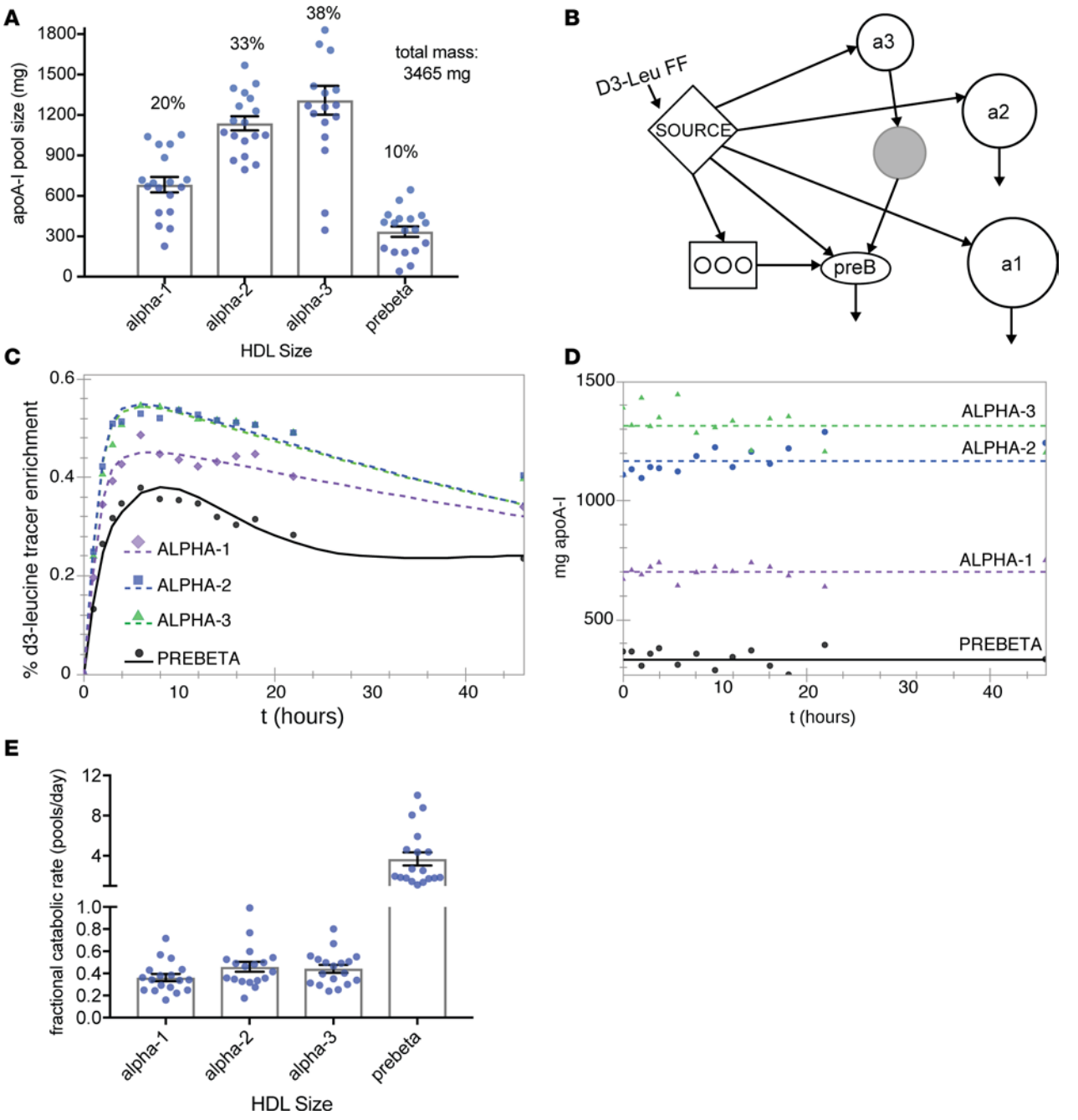

Figure 2. ApoA-I metabolism on 4 sizes of HDL (*n* = 18). (**A**) Mean pool size of plasma apoA-I for 4 sizes of HDL, calculated from SDS-PAGE band densitometry corrected to plasma apoA-I concentrations measured by ELISA. Error bars ± SEM. Numbers above bars show mean percent plasma apoA-I distribution across HDL sizes. (**B**) Compartmental model used in SAAM-II with the greatest parsimony (bare-minimum model). Plasma D3-leucine enrichment, the precursor to protein synthesis, is modeled as a forcing function (FF) input to the liver or intestine ("Source" compartment). Circles represent each HDL size (from large to small: a1 = α-1, a2 = α-2, a3 = α-3, preB = prebeta). Arrows between compartments represent transfer of apoA-I. Arrows out of compartments represent clearance of apoA-I from plasma. The rectangle with interior circles represents an intravascular delay compartment used for synthesis, assembly, and secretion of apoA-I. The gray circle represents a nonsampled remodeling compartment to generate prebeta HDL from α-3 HDL, such as by the action of SR-B1 or hepatic TG lipase. (**C**) SAAM-II model fit of mean tracer enrichment in HDL apoA-I for each HDL size. The tracer enrichments were generated by averaging all participants' enrichments at each time point. (**D**) SAAM-II model fit of mean apoA-I mass (pool size) for each HDL size. The masses were the averages of all participants' masses at each time point. Masses were measured from SDS-PAGE band densitometry corrected to plasma apoA-I concentrations measured by ELISA. (**E**) Mean apoA-I fractional catabolic rates (representing protein turnover) for each HDL size. A value of 0.4 represents 40% of the protein pool turned over each day. Each dot represents a single participant. Error bars ± SEM.

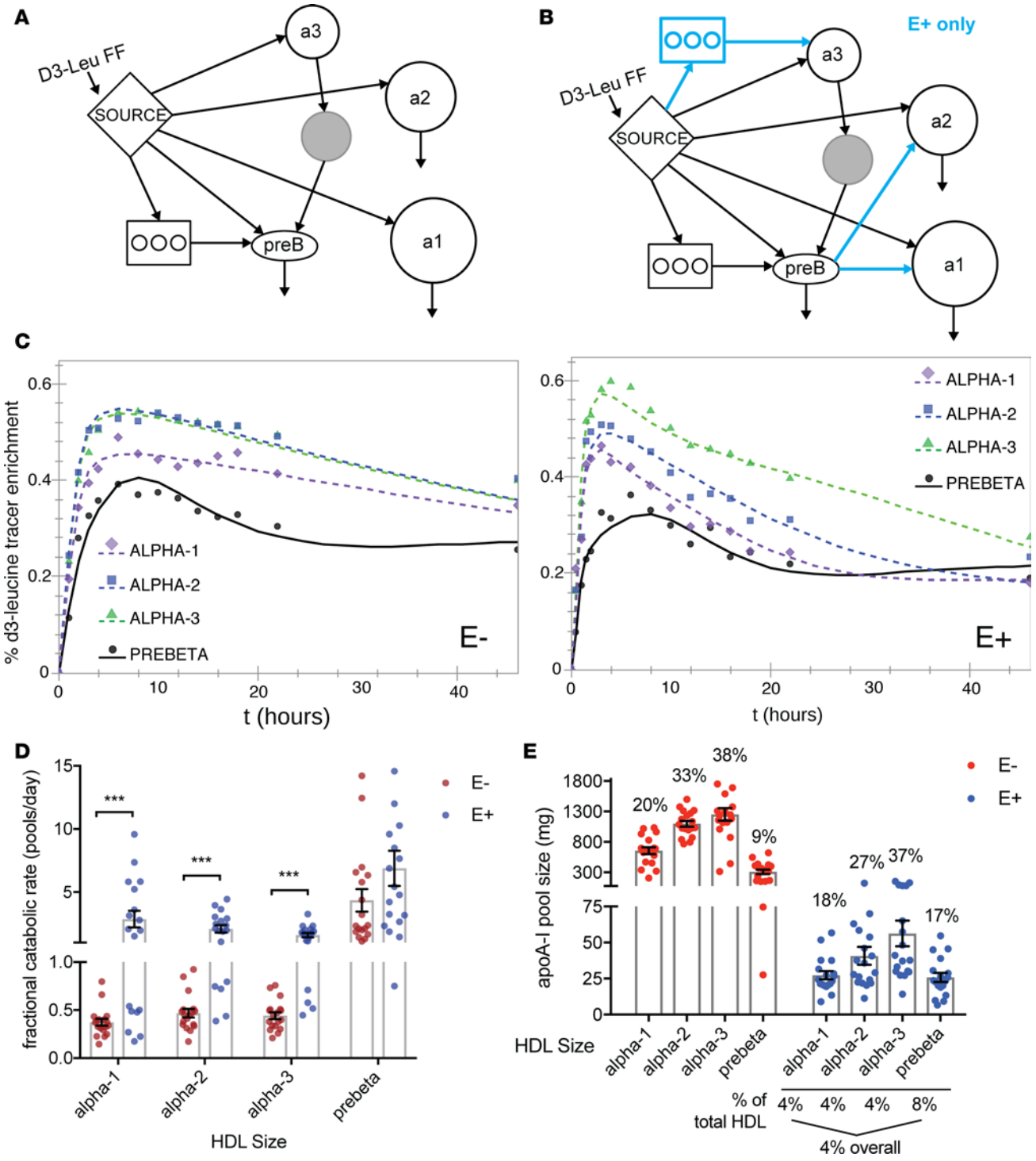

Figure 3. The metabolism of HDL based on presence or absence of apoE (*n* = 18). (**A**) HDL not containing apoE (E^-). Compartmental model used in SAAM-II with the greatest parsimony (bare-minimum model). Plasma D3-leucine enrichment, the precursor to protein synthesis, is modeled as a forcing function (FF) input to the liver or intestine ("Source" compartment). Circles represent each HDL size (from large to small: a1 = α-1, a2 = α-2, a3 = α-3, preB = prebeta). Arrows between compartments represent transfer of apoA-I. Arrows out of compartments represent clearance of apoA-I from plasma. Rectangles with interior circles represent intravascular delay compartments used for lipoprotein synthesis, assembly, and secretion. The gray circle represents a nonsampled remodeling compartment to generate prebeta HDL from α-3 HDL. (**B**) HDL containing apoE (E^+). Modifications to the bare-minimum model from Figure 2A, showing additional size expansion and intravascular delay pathways used in modeling tracer enrichment of apoA-I in HDL containing apoE (E^+) (shown in blue). (**C**) Model fit of apoA-I tracer enrichments in HDL not containing apoE (E^-) (left) and HDL containing apoE (E^+) (right). The tracer enrichments for each HDL size were generated by averaging all participants' enrichments at each time point. (**D**) Mean apoA-I fractional catabolic rates, representing protein turnover, in HDL not containing apoE (E^-) or containing (E^+). Each dot represents a single participant (n = 18). Error bars ± SEM. ***$P < 0.005$ for E^+ vs. E^-, Student's paired 2-sided t test. (**E**) Mean pool sizes (masses) of apoA-I in HDL not containing apoE (E^-) and HDL containing apoE (E^+). Each dot represents a single participant. Numbers above bars represent percent of total pool size (mass) in that subspecies. Bottom right corner shows percent of apoA-I mass on E^+ HDL by size and overall. Error bars ± SEM.

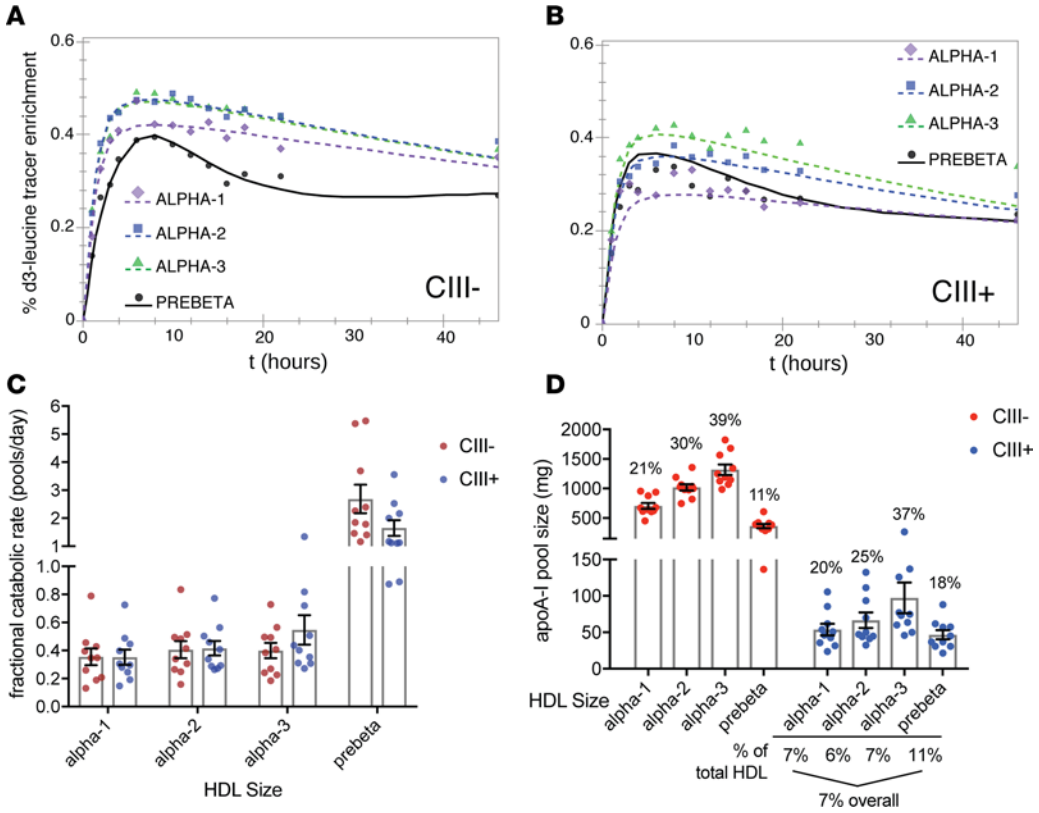

Figure 4. The metabolism of HDL based on presence or absence of apoCIII (*n* = 10). (**A**) Model fit in SAAM-II of average tracer enrichment in HDL not containing apoCIII (CIII$^-$). The tracer enrichments were generated by averaging all participants' enrichments at each time point. The model used was the bare-minimum model (Figure 2A). (**B**) Model fit in SAAM-II of average tracer enrichment in HDL containing apoCIII (CIII$^+$). The tracer enrichments were generated by averaging all participants' enrichments at each time point. The model used was the bare-minimum model (Figure 2A). (**C**) Mean plasma apoA-I fractional catabolic rates on HDL not containing apoCIII (CIII$^-$) and containing apoCIII (CIII$^+$). Each dot represents a single participant. Error bars ± SEM. All comparisons between sizes not significant ($P > 0.05$) by Student's paired 2-sided *t* test. (**D**) Mean pool sizes of apoA-I in HDL not containing apoCIII (CIII$^-$) and HDL containing apoCIII (CIII$^+$). Each dot represents an individual participant. Numbers above bars represent percent of total pool size in that subspecies. Bottom right corner shows percent of apoA-I mass on CIII$^+$ HDL by size and overall. Error bars ± SEM.

Figure 3C). Corroborating these visual findings, the apoA-I FCRs shown in Figure 4C and summarized in Supplemental Table 1 were not significantly different between CIII$^-$ and CIII$^+$ HDL (*P* value for 2-tailed paired *t* test not significant across each size) and were similar to those of plasma apoA-I and E$^-$ HDL (Figure 2E, Figure 3D). As with the E$^+$ subspecies, a small percentage of apoA-I resides on HDL that contains apoCIII, and the size distributions for apoA-I on CIII$^+$ and CIII$^-$ HDL were relatively similar (Figure 4D). Taken together, these results demonstrated no clear difference in apoA-I metabolism between HDL containing apoCIII and HDL not containing apoCIII.

HDL speciation according to presence of apoE and/or apoCIII. Because we hypothesized that apoE and CIII have antagonistic effects on HDL metabolism, we studied the metabolism of apoA-I on the 4 subspecies with and without apoE and/or apoCIII: E$^-$CIII$^-$, E$^+$CIII$^-$, E$^-$CIII$^+$, and E$^+$CIII$^+$. Figure 5 describes the distribution of apoA-I mass and secretion across the 4 subspecies each separated into 4 sizes. The majority of apoA-I mass was in E$^-$CIII$^-$ HDL (91%), followed by 6% in E$^-$CIII$^+$, 2% in E$^+$CIII$^-$, and 1% in E$^+$CIII$^+$ (Figure 5A). Consistent with these values, the majority of HDL-C is found on E$^-$CIII$^-$ HDL (82%), followed by 8% in E$^-$CIII$^+$, 5% in E$^+$CIII$^-$, and 5% in E$^+$CIII$^+$ (Table 2). The intrasubspecies size distribution was roughly similar across the subspecies, except for E$^+$CIII$^+$, which had a disproportionate amount of apoA-I on prebeta (33% of E$^+$CIII$^+$ mass vs. 16% of E$^+$CIII$^-$, 14% of E$^-$CIII$^+$, and 11% of E$^-$CIII$^-$). The majority of apoA-I was secreted on E$^-$CIII$^-$ HDL (86%), consistent with its large pool size (Figure 5B). E$^-$CIII$^+$ received 5% of total apoA-I secretion, E$^+$CIII$^-$ received 6%, and E$^+$CIII$^+$ received 3%. The percent distribution of apoA-I secretion onto each size was similar by subspecies, with α-2 and α-3 HDL having the most apoA-I synthesis per day. E$^+$CIII$^-$ HDL had a disproportionate amount of apoA-I secretion (6% of total apoA-I secretion vs. 2% of total apoA-I mass), as did E$^+$CIII$^+$ (3% of total apoA-I secretion vs. 1% of total apoA-I

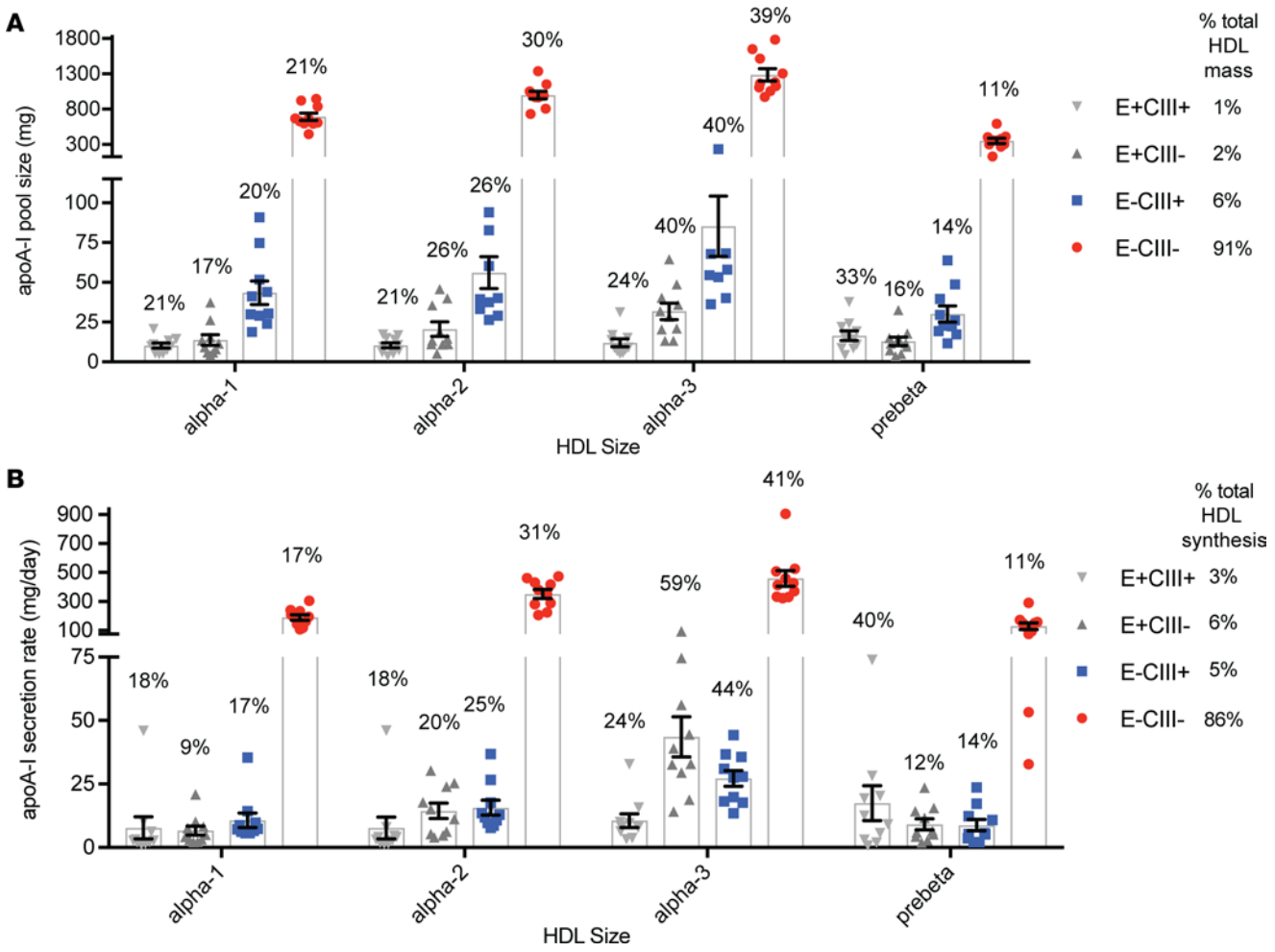

Figure 5. Plasma pool size and secretion rates of HDL subspecies containing apoE and/or apoCIII (*n* = 10). (**A**) Mean plasma apoA-I pool size, calculated by SDS-PAGE densitometry corrected to plasma apoA-I concentrations measured by ELISA. Each point represents an individual participant. Numbers over bars represent the percent of pool size for each subspecies. Error bars ± SEM. Right, percent of total HDL mass. E^+CIII^+, HDL containing apoE and apoCIII; E^+CIII^-, HDL containing apoE but not apoCIII; E^-CIII^+, HDL containing apoCIII but not apoE; E^-CIII^-, HDL not containing apoE or apoCIII. (**B**) Mean plasma apoA-I secretion rates in 4 HDL subspecies defined by presence or absence of apoE or apoCIII, determined by SAAM-II modeling software. Each point represents an individual participant. Numbers over bars represent the percent of total apoA-I secretion (synthesis) for each subspecies. Error bars ± SEM. Right, percent of total HDL secretion (synthesis).

mass). Supplemental Figure 1 illustrates these model-derived rates and pool sizes for the 4 HDL subspecies divided into 4 sizes. We also calculated molar ratios of apolipoproteins on each HDL subspecies, aggregating all sizes together. There was about 1 apoE to each apoA-I on E^+CIII^-, 2 apoCIII per apoA-I on E^-CIII^+, and about 2.5 apoE and 5 apoCIII per apoA-I on E^+CIII^+. These values are consistent with what has been reported previously in a separate group of participants (9).

We then modeled the apoA-I tracer enrichment in each subspecies, using the average enrichment data of 10 participants (Figure 6A). Tracer enrichments of apoA-I in all sizes and subspecies of HDL appeared in circulation at about the same time, as we reported previously (41). In all subspecies, tracer enrichment of apoA-I in the smallest prebeta HDL peaked later than the larger α sizes, indicating that prebeta could not be a pure precursor to any larger HDL, a major principle of reverse cholesterol transport. Notably, apoA-I in the E^+CIII^- subspecies had faster rises and steeper descending slopes in tracer enrichments compared with the other subspecies, suggestive of faster HDL turnover.

The final models used in SAAM-II are shown in Figure 3, A and B. The model with the greatest parsimony, the bare-minimum model, is characterized by direct secretion of all HDL sizes from the source compartment, an intravascular delay compartment for the prebeta fraction, no size conversion of a smaller to a larger HDL, and size contraction only from α-3 to prebeta HDL (Figure 3A). This model had satisfactory visual fit

Table 2. Concentration, percent distribution, and mass ratios of HDL-C and apoA-I across 4 HDL subspecies (n = 10)

	HDL-C (mg/dl)				apoA-I (mg/dl)				HDL-C: apoA-I ratio
	Mean	SEM	% of total	SEM	Mean	SEM	% of total	SEM	
E^-CIII^-	33	3	82%	7%	101	7	91%	6%	0.3
E^-CIII^+	3	0.3	8%	1%	6	1	6%	1%	0.5
E^+CIII^-	2	0.2	5%	0.5%	2	0.4	2%	0.4%	0.8
E^+CIII^+	2	0.2	5%	0.4%	1	0.2	1%	0.1%	1.3
Sum	40		100%		112		100%		0.4

and was statistically suitable (the majority of parameter values estimated by SAAM-II had 95% CI excluding zero) for all subspecies and sizes except for the E^+CIII^-, which required a more complex model (Figure 3B). This subspecies uniquely required size expansion pathways from prebeta HDL to α-2 and α-1 to fit the data. These size expansion pathways both improved the visual fit and reduced the weighted residual sum of squares (WRSS) enough to justify their addition, as determined by a significant result by F test (Figure 7). The final models also had excellent apoA-I mass fits, and the masses from SAAM-II modeling correlated highly to those measured in SDS-PAGE band quantification (Supplemental Figure 2). Model development is described in detail in the Supplemental Methods.

FCRs. After establishing the final models using the average tracer enrichment and pool sizes of 10 participants, we then modeled the apoA-I tracer enrichment and pool sizes of each participant in the study to calculate clearance rates (Figure 6B). Uniquely, apoA-I on E^+CIII^- was cleared 2–11 times faster than E^-CIII^-, E^-CIII^+, and E^+CIII^+ depending on the size ($P < 0.001$ for all comparisons). These accelerated turnover rates contributed to the disproportionately greater flux of apoA-I in the E^+CIII^- subspecies relative to its share of the apoA-I pool size (Figure 5, A and B). Importantly, FCRs for apoA-I on E^+CIII^+ were significantly slower than on E^+CIII^-. E^+CIII^+ had slightly faster turnover rates than on E^-CIII^+ and E^-CIII^-, though it was only significant in the small α-3 size. FCRs for apoA-I on E^-CIII^- and E^-CIII^+ were similar. Altogether, these results demonstrate an interaction between apoE and apoCIII on the clearance rate of HDL apoA-I.

Subgroup analyses. Supplemental Table 2 is a breakdown of apoA-I FCR, pool size, and flux in each subspecies by sex, race, apoE genotype, and BMI (overweight vs. obese). We did not test for statistical significance due to small sample size, but we report the following potentially interesting findings: the average male apoA-I FCR was higher than the average female apoA-I FCR, and the apoE2/E4 genotype had lower apoA-I clearance rates than apoE3/E3 in the E^+ subspecies.

Association of apoE in HDL containing or not containing apoCIII and risk for CHD. We then wanted to determine if differences in metabolism among these HDL subspecies corresponded to differences in risk of CHD. We used a case-cohort study nested within the Danish DCH study including 1,750 participants selected randomly at baseline and 1,946 participants with incident CHD cases during a median follow-up of 9 years (Table 1). The median levels of apoA-I in each HDL subspecies were not different in the random subcohort versus in the participants who developed CHD, and the concentration of apoE in each HDL subspecies correlated moderately with other lipoprotein measurements (Supplemental Table 3). In multivariable adjusted regression analysis, the concentration of apoE in unfractionated HDL was not statistically significantly associated with CHD risk (Supplemental Table 4). The hazard ratio (HR) for CHD across extreme quintiles of apoE in unfractionated HDL was 0.97 (95% CI, 0.66–1.41; P [trend] = 0.88). Next, we investigated if the concentration of apoE in separate subspecies of HDL containing or not containing apoCIII was differentially related to incident CHD (Figure 8 and Supplemental Table 4). In multivariable regression analysis, adjusting for potential confounders, the risk for CHD across extreme quintiles of apoE in HDL that contained apoCIII was not statistically significantly higher (HR 1.29 [95% CI, 0.86–1.93]; P [trend] = 0.25). In contrast, in HDL not containing apoCIII, the concentration of apoE was inversely related to risk of CHD. The risk of CHD was 34% lower in participants in the highest quintile compared with participants in the lowest quintile of apoE levels in the subspecies of HDL not containing apoCIII (HR 0.66 [95% CI, 0.48–0.89]; P [trend] = 0.01). The regression coefficients of apoE in the 2 HDL subspecies containing and not containing apoCIII and CHD risk were statistically significantly different (P [heterogeneity] = 0.02).

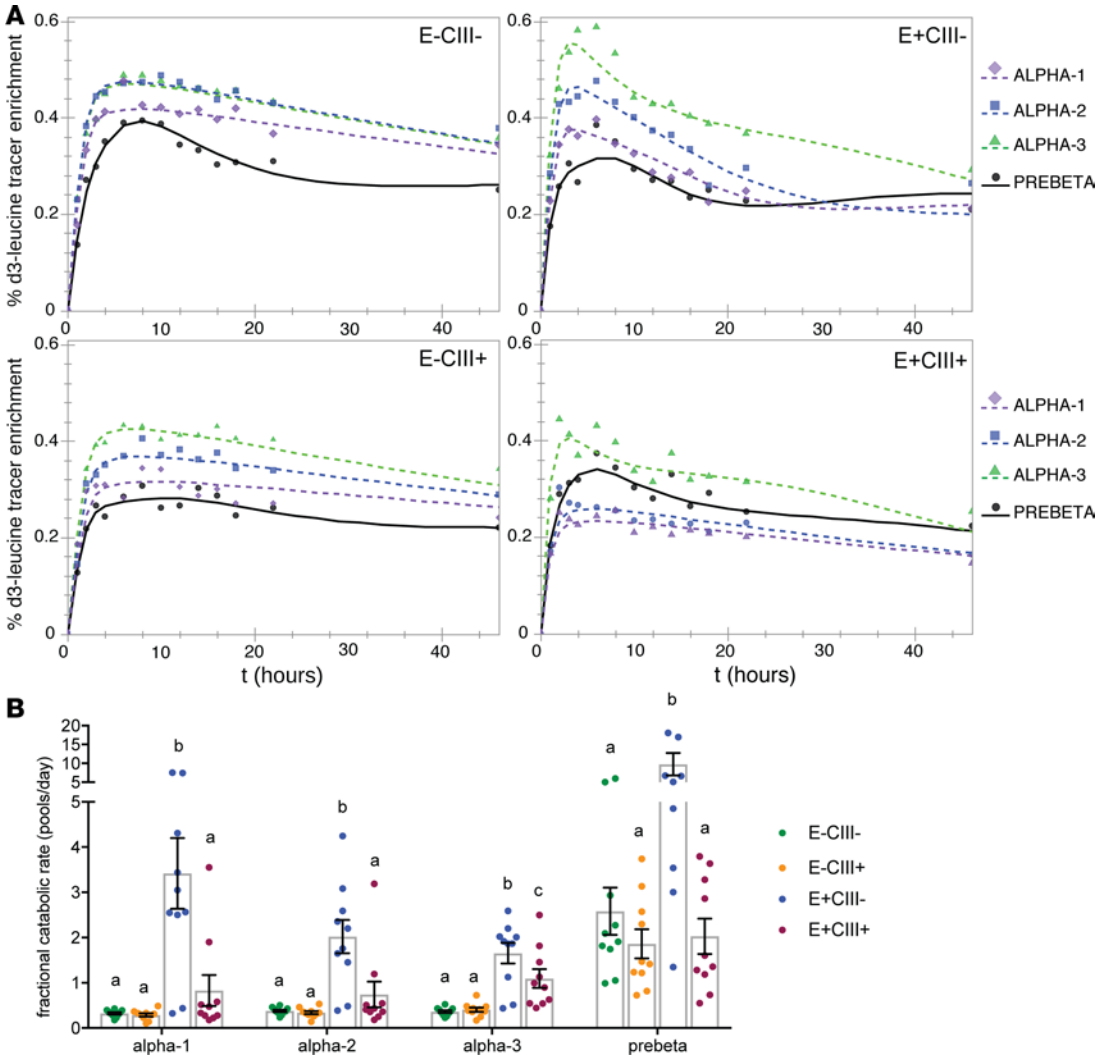

Figure 6. Interaction between apoE and apoCIII on HDL. Model fit for apoA-I tracer enrichments and apoA-I FCRs (pools/day) in 4 HDL subspecies each separated into 4 HDL sizes (n = 10). (**A**) Model fit and mean tracer enrichments. The % D3-leucine tracer enrichments (D3-leucine/[D3-leucine + unlabeled leucine] × 100) were computed by averaging all participants' enrichments (n = 10) at each time point and modeling them as a single participant. The bare-minimum model, as shown in Figure 2A, was used for E^-CIII^-, E^-CIII^+, and E^+CIII^+. The complex model, as shown in Figure 2B, was used for E^+CIII^- only. (**B**) ApoA-I fractional catabolic rates, representing protein turnover. Each point represents a single participant (n = 10). A value of 1 = 100% of protein pool turned over per day. Error bars ± SEM. Within each HDL size, different letters above each bar refer to statistically different mean values ($P < 0.005$ vs. all other subspecies as assessed by mixed effects model). Specifically, the FCR of E^+CIII^- subspecies in each size is significantly faster than that of the other subspecies, whereas the FCR of E^+CIII^+ is not significantly higher, suggesting an interaction between the 2 apolipoproteins on HDL. One outlier is not shown for visual purposes (E^+CIII^- prebeta, value 31 pools/day) but was included in the statistical analysis.

Additional adjustment for factors involved in the pathophysiology of CHD including HDL–apoA-I, apoCIII, plasma triglycerides, and apoB (Supplemental Table 4) did not affect the results. ApoE in total (unfractionated) HDL was unrelated to risk of CHD (P [trend] = 0.79). The concentration of apoE in HDL was inversely associated with CHD risk only in HDL not containing apoCIII (P [trend] = 0.02 in HDL containing apoCIII versus P = 0.86 in HDL not containing apoCIII).

Discussion

This study is the first to our knowledge in humans to link the impact of an apolipoprotein on HDL physiology to risk of CHD. The central metabolic findings are that a subspecies of HDL that contains apoE but not apoCIII uniquely participates in classical pathways of reverse cholesterol transport: disproportionately high secretion into plasma, size expansion most likely achieved by taking up cholesterol (the major lipid component of the HDL core), size contraction achieved at least in part by selective cholesterol ester uptake

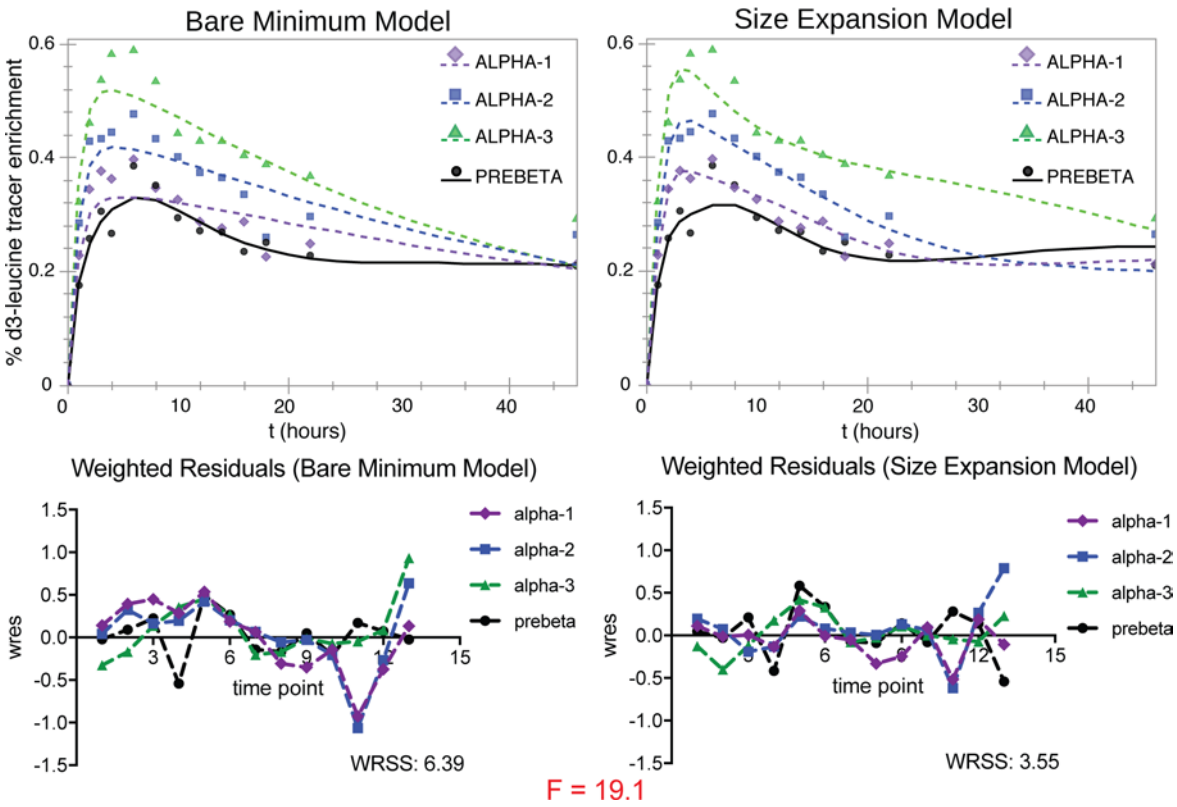

Figure 7. Justification for use of a more complex model that includes size expansion for the HDL E^+CIII^- subspecies. Shown are model fits of the average apoA-I tracer enrichments in HDL E^+CIII^-, using the bare-minimum model (left, shown in Figure 2A) vs. complex model featuring size expansion (right, shown in Figure 2B) (n = 10). Weighted residuals (wres) for each time point (13 in total, 1 hour to 46 hours) are shown below with WRSS and value for F-statistic (comparison of models: $P < 0.001$). The highly significantly lower WRSS for the size expansion model used for HDL E^+CIII^- indicates that the additional pathways for size expansion are needed to optimize the fit of the model to the data.

by the liver and potentially via actions of lipoprotein lipase (LPL) and hepatic lipase (HL) to generate prebeta HDL, and increased clearance rates from the circulation. These pathways are not evident for HDL that does not contain apoE. We also found that apoCIII robustly attenuates the size expansion pathway and high clearance rate.

We interpreted the metabolic results to mean greater reverse cholesterol transport for only the HDL subspecies that contains apoE but not apoCIII. Next, we studied whether these metabolic indicators of reverse cholesterol transport corresponded to lower rates of clinical CHD outcomes for HDL containing apoE, which might be attenuated when apoCIII is also present. The results of the epidemiology study match the metabolism study closely. In a large prospective population-based study, the apoE concentration of HDL is inversely related to the risk of CHD but only in the major HDL subspecies that does not contain apoCIII (Figure 8). Interestingly, early work by Mahley and colleagues (44) showed that increasing the amount of apoE in phospholipid disks exponentially increased their affinity for LDL receptors on human fibroblasts, which provides an additional mechanistic explanation for these findings. In contrast, the apoE concentration was not associated with CHD in the subspecies of HDL that contains apoCIII, indicating that no amount of apoE in a physiological range can overcome the effect of the apoCIII also present. We demonstrate for the first time to our knowledge a close correspondence between metabolic properties of HDL subspecies, defined by specific protein content that presumptively affects reverse cholesterol transport, and the prediction by these HDL subspecies and proteins of risk of CHD in a population (Figure 9).

We found disproportionate apoA-I secretion and HDL-C content in E^+CIII^- and E^+CIII^+ HDL relative to their respective pool sizes (Figure 3B and Table 2). This disproportionate flux in synthesis is supported by the ability of apoE to activate ABCA1 (45, 46), which is present on hepatocytes and is an essential mediator in HDL biogenesis. This has also been studied in a mimetic peptide derived from the C-terminal domain of apoE, which stimulated ABCA1-mediated efflux from cultured macrophages and nascent HDL

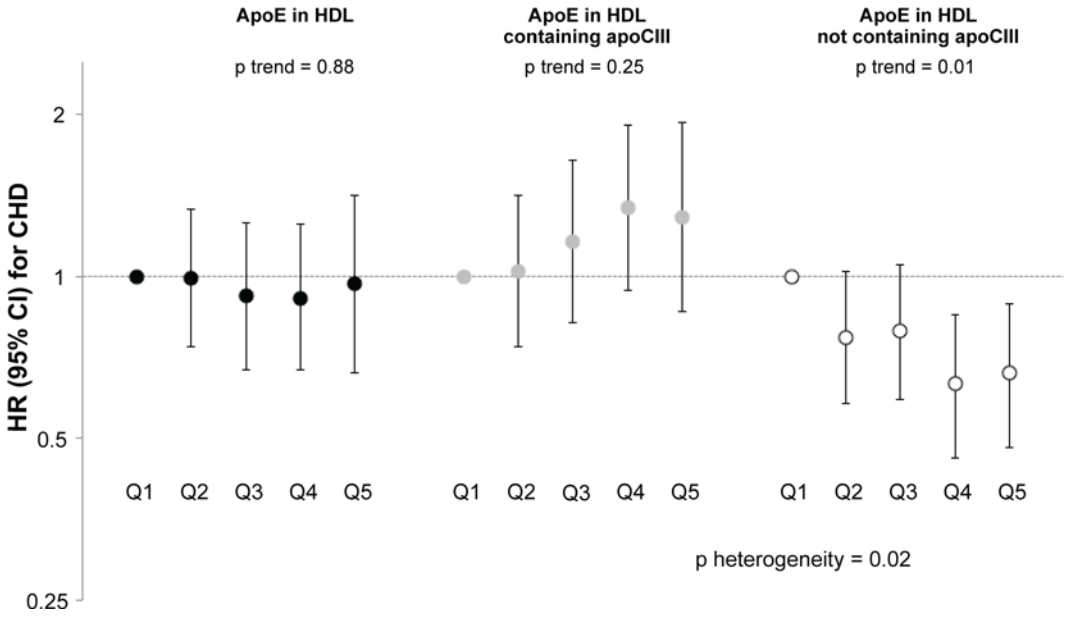

Figure 8. HDL apoE and apoCIII interact with coronary heart disease (CHD). The concentration of HDL was quantified by apoA-I levels. Hazard Ratios (HRs) and 95% CI of CHD are shown according to quintiles of apoE concentration in unfractionated HDL and in HDL containing or not containing apoCIII in participants of the Danish DCH study (*n* = 3,635). HRs were adjusted for laboratory batch, smoking status (never; former; current <15, 15–24, ≥25 g/day), education (missing, <8; 8–10; >10 years), alcohol intake (nondrinker; drinker <5, 5–9, 10–19, 20–39, ≥40 g/alcohol/day), BMI (<25; 25–<30; >30 kg/m^2), self-reported diagnosis of hypertension, and self-reported diagnosis of diabetes at baseline obtained from Cox proportional hazard regression models, with standard inverse probability weights and age used as underlying time scale and stratification by sex. ApoE concentration in HDL containing or not containing apoCIII were simultaneously included in the model. Equality of the regression coefficients was tested for apoE in HDL containing apoCIII and apoE in HDL not containing apoCIII (*P* [heterogeneity] = 0.02). The significant heterogeneity test indicates that the association with CHD is different for HDL apoE concentration depending on the presence or absence of apoCIII on the HDL.

formation (47). Furthermore, LPL could contribute to the formation of HDL by transferring surface protein and lipid from remnant chylomicrons and VLDL to newly synthesized HDL particles (48, 49).

Our models suggest that HDL containing apoE participates in size expansion of HDL more so than HDL that does not contain apoE, likely due to increased cholesterol incorporation into the core of the particle, which is supported and confirmed by evidence in vitro and in animal models. Structural investigations have shown that apoE has a different conformation on HDL than does apoA-I and that this conformation facilitates lipid incorporation into the particle (21, 45, 50). ApoA-I–containing HDL from CETP-deficient humans is able to accommodate only a limited amount of cholesterol ester, which is greatly increased when apoE is present (51). In mice lacking apoA-I, adenoviral-mediated expression of apoE promoted the secretion of discoidal HDL, which was converted to spherical (α) HDL by lecithin-cholesterol acyl transferase (LCAT), indicating size expansion (22). In canine serum depleted of apoE, coincubation of cholesterol-loaded J774 macrophages with exogenous human apoA-I modestly increased the concentration of all sizes of HDL, whereas exogenous apoE robustly increased mainly larger HDL, again potentially reflecting size expansion. Of note, incubation with exogenous human apoCIII did not result in an increase in concentration of any HDL size (19). Our results support these findings, given that we saw evidence of size expansion in E^+CIII^- HDL, but not in E^-CIII^+ or E^+CIII^+ (Figure 7 and Supplemental Methods).

Consistent with the role of apoE as a high-affinity liver receptor ligand (13, 15, 52), we found that the subspecies of HDL containing apoE has a much shorter residence time in the circulation than the subspecies of HDL that does not contain apoE, about 8 hours compared with 2.5 days, with the assumption that apoA-I kinetics recapitulate HDL particle kinetics (Figure 3D). The 8-hour residence time for apoA-I HDL containing apoE is similar to the residence time of apoE itself on HDL (53), suggesting apoE mediates holoparticle uptake and complete removal of the HDL particle on which it resides. HDL containing apoE could also interact with circulating HL to increase hydrolysis of HDL phospholipid and triglyceride to regenerate prebeta HDL (54).

Unlike apoE, apoCIII appears to have a minor role, if any, in apoA-I metabolism on its own, given that the metabolism of apoA-I on $CIII^+$ HDL is similar to $CIII^-$ HDL (Figure 4 and Supplemental Table 1) and the metabolism of apoA-I on $CIII^+$ HDL is similar to E^-CIII^- (Figure 6 and Supplemental Table 1).

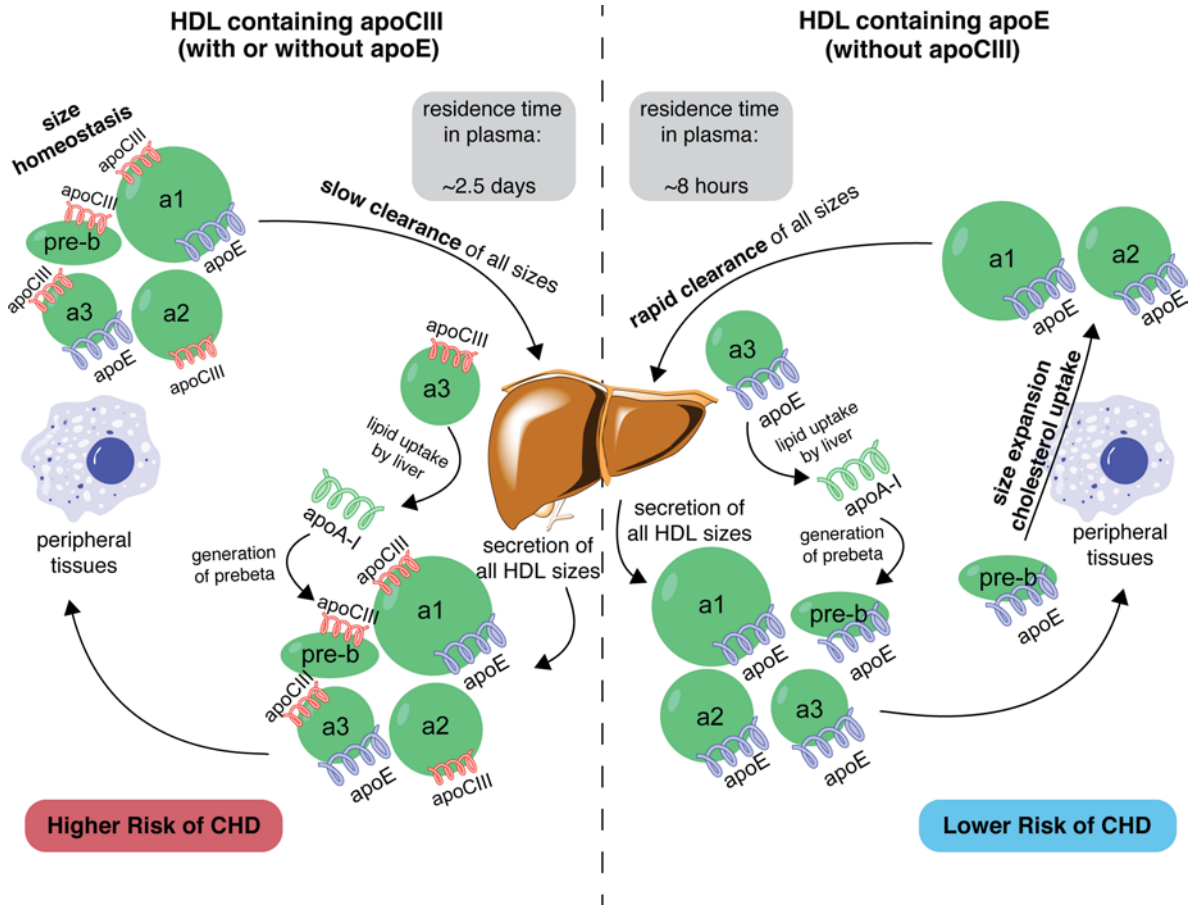

Figure 9. Integrated model of HDL metabolism and epidemiology showing an adverse interaction between apoE and apoCIII. Left panel: The liver secretes HDL containing both apoE and apoCIII (E^+CIII^+) or HDL containing apoCIII but not apoE (E^-CIII^+) across a range of HDL sizes. These HDL subspecies do not experience significant size expansion that increases the size category. Upon arrival at the liver, either the lipids are cleared and prebeta generated, or the particles are cleared slowly from circulation (residence time: approximately 2.5 days). These HDL subspecies are associated with a higher risk of CHD. Right panel: The liver secretes HDL containing apoE but not apoCIII (E^+CIII^-) across a range of sizes. This HDL subspecies experiences size expansion from discoidal prebeta to larger α sizes, due to efflux of cholesterol from peripheral tissues. Upon arrival at the liver, either the lipids are cleared and prebeta generated, or the particles are cleared rapidly from the circulation (residence time: ~8 hours). This HDL subspecies is associated with a lower risk of CHD.

Importantly, however, the presence of apoCIII strongly abolishes the effect of apoE to increase clearance of HDL, as shown by comparing FCR in E^+CIII^+ compared with E^+CIII^- (Figure 6B). These opposing roles of apoE and apoCIII in humans have been shown in apoB-containing lipoproteins, in which E^+CIII^- VLDL and IDL are cleared rapidly, but E^+CIII^+ VLDL and IDL have attenuated clearance rates, although faster than E^-CIII^+ (17, 30, 36). This antagonistic effect has also been shown mechanistically in vitro (28, 32) and in animal models (33–35), in which exogenous or transgenic apoE is able to facilitate lipoprotein binding to LDL-R and lipoprotein uptake, and exogenous or transgenic apoCIII ablates this effect. Taken together, the effect of apoCIII on HDL metabolism manifests only when apoCIII coexists with apoE on HDL.

The metabolic evidence here supports and is supported by epidemiological evidence suggesting that apoCIII interferes with antiatherogenic functions of HDL. When human HDL is separated into subspecies containing or not containing apoCIII, the concentration of HDL that contains apoCIII predicts higher risk of CHD, whereas HDL that does not contain apoCIII predicts lower risk (40, 55). In our study, the inverse association of apoE in HDL with the risk of CHD was completely masked in HDL that contains apoCIII (Figure 8 and Supplemental Table 4). Findings from studies on the association of apoE in unfractionated HDL and CVD have been inconsistent. In a prospective nested case-control study (370 control participants, 418 cases) in a randomized, placebo-controlled clinical trial of pravastatin in survivors of myocardial infarction (MI), higher concentrations of apoE in HDL were associated with an increased risk for recurrent coronary events (38). In a cross-sectional setting, there were reduced levels of apoE in HDL isolated from the plasma of 40 CAD patients compared with 20 healthy subjects (56). In contrast, a clinical study revealed

higher concentrations of apoE in a small and dense subfraction of HDL (HDL_3) from 7 patients with CAD compared with HDL_3 of 6 healthy controls (37). Similarly, higher apoE levels in HDL were observed in 74 male coronary bypass patients compared with 78 apparently healthy male controls (57). These divergent results might be related to small sample sizes of some of the studies, cross-sectional study design, and lacking adjustment for potential confounders. As the concentration of apoE or apoCIII in HDL might be influenced by disease status, it is particularly important to study this association in prospective studies in populations without CHD at baseline, as we did for the first time to our knowledge in the present study.

Strengths of our metabolic study include large sample size for a kinetic study, wide age range of study participants, and inclusion of men and women as well as white and black participants. Restriction of the study population to the low-HDL, high-BMI phenotype, frequently seen with the metabolic syndrome, is clinically relevant but restricts our ability to make conclusions about HDL metabolism in individuals with optimal body weight and high HDL-C. We restricted the use of medications that alter HDL levels (e.g., statins, estrogen replacement therapy) to ensure these were not study confounders. Our study participants received a high–unsaturated fat diet easy to adhere to with foods typical of the US population. Strengths of the prospective case-cohort study include the large sample size with minimal loss to follow-up, the population-based design, and the rigorous validation of CHD cases. Another cost-efficient study design often used to minimize the use of precious biological samples, but retaining the prospective setting, is the nested case-control design where matching of future cases to controls who remain free of disease can take care of important confounders such as smoking and age at the design phase. The main advantage of the present case-cohort study design is that the random subcohort can be used as a comparison group for multiple outcomes (58). In case-cohort studies, potential confounding must be addressed by comprehensive multivariable adjustments. A recent study showed that both designs yield comparable results to full cohort analyses, especially if inverse probability weighting is applied (59). Our study extends the ongoing discussion about HDL heterogeneity and provides evidence that apoE is involved in HDL's cardioprotective activities. Unfortunately, no apoE genotype data were available for this analysis, and future studies should evaluate if apoE isoforms provide further insight in the association of apoE in HDL and risk of CHD. However, the proportion of HDL carrying apoE did not differ by apoE genotype in a previous study (39).

This study in humans is the first to our knowledge to show that apolipoproteins, present at small concentrations in HDL, can strongly influence the metabolism of HDL in plasma and interact to affect CHD risk. A unique subspecies of HDL that contains apoE but not apoCIII behaves entirely differently from other HDL. High secretion, coupled with size expansion and rapid clearance, of HDL containing apoE but not apoCIII suggests an HDL particle especially active in reverse cholesterol transport hypothesized to protect against atherosclerosis and points to a potential therapeutic target. However, apoE on HDL is unable to overcome the metabolic influence of apoCIII also present on HDL. These metabolic findings map closely with our finding that HDL apoE is associated with lower CHD risk, but only so on HDL that does not contain apoCIII, and is ineffective when apoCIII is present. It is important to note that we only studied this subspecies in overweight and obese individuals with low HDL-C, where the concentration of E^+CIII^- HDL is quite low in plasma. It is plausible that lean, healthy individuals with presumably higher HDL functionality have greater amounts of E^+CIII^- HDL. HDL subspecies, because they are based on functional properties of the associated proteins, are more likely to have a causal role in atherosclerosis and CHD events and should be explored in further studies.

Methods

Study population and design. For the metabolic study, we recruited adults between 23 and 70 years old who had low HDL-C (<45 mg/dl for men, <55 mg/dl for women) and high BMI (25–35 kg/m^2). Exclusion criteria included HDL-C (<20 mg/dl), LDL-C (>160 mg/dl), TG (>500 mg/dl), use of lipid-lowering medications or hormone replacement therapy, diabetes, and E2/E2 or E4/E4 apoE genotypes. In total, 63 individuals were screened, 24 completed part or all of the study, and 18 were analyzed.

The association of apoE in HDL and incident CHD was investigated in 3,639 participants that were part of a previous case-cohort study nested in the in the Danish DCH study (60). As described in detail previously, the DCH study is an ongoing prospective study initiated in 1993–1997 when 57,053 Danish-born residents, aged 50–65 years without record of cancer diagnosis in the Danish Cancer Registry, participated in a clinical examination and detailed lifestyle survey.

This case-cohort study included all confirmed-incident cases of CHD between study entry and May 2008 (n = 2,063) and a random subcohort (n = 1,824) of individuals from the original DCH cohort who were free of CHD at baseline. After exclusion of participants for whom information on our main biochemical exposures was missing, the case-cohort included 1,946 participants with incident CHD and 1,750 participants of the random subcohort. Due to the case-cohort design, 57 participants with incident CHD are also part of the random subcohort.

The baseline examination included anthropometric and blood pressure measurements performed by trained Brigham and Women's Hospital laboratory technicians. Participants completed self-administered questionnaires requesting information on participant's age, sex, years of education, smoking status, alcohol consumption, and history of hypertension and diabetes. Average alcohol consumption over the previous year (g/d) was calculated based on reported alcoholic beverages (beer, wine, spirits, and mixed drinks) assessed with a validated food-frequency questionnaire mailed to the study participants before the visit to the study center. Blood was sampled at baseline in the study clinics in Aarhus and Copenhagen, and plasma samples were stored at −150°C.

Dietary protocol. The participants of the metabolic study received a healthy high–unsaturated fat diet (45% carbohydrate, 40% fat [10% saturated, 23% monounsaturated, 7% polyunsaturated], 15% protein, 180 mg cholesterol per day) for 28 days prior to the kinetic study. The diet was formulated by the Center for Clinical Investigation nutrition research unit of Brigham and Women's Hospital. Participants picked up all their food to take home on Monday, Wednesday, and Friday at the study site. All food and beverages were provided, and participants were not allowed to eat any other food, but they were allowed diet soda, coffee, and tea. Alcoholic beverages were not included or permitted. Physical activity was not monitored, but participants were asked not to alter their usual physical-activity pattern. Participants were weighed during food pickups, and dietitians adjusted the amount of food to prevent changes in weight. These procedures have been used in our previous studies (17, 30, 41).

Infusion protocol. On the morning of day 29, participants in the metabolic study were admitted to the Clinical and Translational Science Center (CTSC) at Brigham and Women's Hospital. Participants were given i.v. a bolus of (5,5,5-D3) L-leucine (Cambridge Isotope Laboratories, Cambridge, Massachusetts, USA) at a dose of 10 mg/kg, administered in a volume of 150 ml at 15 ml/minute. Blood was sampled at 0, 0.5, 1, 1.5, 2, 3, 4, 6, 8, 10, 12, 14, 16, 18, 22, 46, 70, and 94 hours after infusion into chilled tubes that had been stored in the cold room (4°C). Plasma was separated immediately in a refrigerated centrifuge and aliquoted into tubes containing phenylmethanesulfonyl fluoride, gentamicin, benzamidine, and a protease inhibitor cocktail (all from MilliporeSigma). Aliquots were stored at –80°C until lipoprotein separation began after a mean time of 12 months (range 1–24 months).

HDL subspecies separation using immunoaffinity column chromatography. These methods have been described in detail (9). Briefly, thawed plasma from each time point was incubated with Sepharose 4B immunoaffinity columns (Bio-Rad) containing affinity purified polyclonal antibodies to apoA-I (catalog 11A-G2b, Academy Bio-Medical Co.). The apoA-I–containing bound lipoproteins were eluted with 3M sodium thiocyanate and were immediately desalted in PBS. This procedure was repeated with the unbound lipoproteins to improve recovery of apoA-I. Then, apoA-I–containing lipoproteins were incubated in an anti-apoE immunoaffinity column (Academy Bio-Medical Co.) to separate HDL into 2 subspecies: HDL not containing apoE (E^-), and HDL containing apoE (E^+). In the last 10 participants, an additional immunoaffinity separation using anti-apoCIII (anti-apoE, catalog 50A-G1b; anti-apoCIII, catalog 33A-R1b; both from Academy Bio-Medical Co.) columns produced 4 subspecies: HDL not containing apoE or apoCIII (E^-CIII^-), HDL containing apoCIII but not apoE (E^-CIII^+), HDL containing apoE but not apoCIII (E^+CIII^-), and HDL containing both apoE and apoCIII (E^+CIII^+). Repeat incubation of unbound HDL to apoE or apoCIII columns was not needed. Efficiency of columns was measured and determined to be 90% for apoA-I, 99% for apoE, and 98%–99% for apoCIII. There were no differences in size or subspecies distribution comparing the HDL that bound to the anti–apoA-I antibody resin and that which did not.

HDL size separation and apoA-I purification. These methods have been described in detail (41). Briefly, HDL subspecies were separated by size using nondenaturing PAGE on a 4%–30% gradient gel (Jule Biotechnologies) into 4 sizes: α-1 (9.5–12.2 nm), α-2 (8.2–9.5 nm), α-3 (7.1–8.2 nm), and prebeta (<7.1 nm) and then electrophoretically transferred to a 0.45 μm PVDF membrane (GE Life Sciences). The membranes were then stained with 0.2% amido black (MilliporeSigma). HDL of each size were excised from PVDF membranes and eluted overnight at 4°C in Tris-SDS-Triton-X (JT Baker, MilliporeSigma, Bio-Rad, respectively). ApoA-I from each HDL size was purified using SDS-PAGE in a 4%–20% gradient, transferred to

a PVDF membrane, and stained with 0.2% amido black. Excised apoA-I bands underwent amino acid hydrolysis and derivitization to heptafluorobutyric acid esters. Measurements of tracer enrichment were performed by gas chromatography/single-ion monitoring mass spectrometry as previously described (17).

Tracer enrichment and pool size. The apoA-I tracer enrichment at each time point was defined as AUC of D3-leucine/(AUC of D3-leucine + AUC of d0-leucine). ApoA-I concentration of each HDL subspecies was measured at each time point using SDS-PAGE band densitometry, corrected to plasma total apoA-I values determined by ELISA. ApoA-I pool size was determined by multiplying apoA-I concentration by plasma volume, which was assumed to be 4.4% of ideal body weight (calculated by using a BMI of 25 kg/m^2). Because all participants were overweight, we adjusted the plasma volume using the following formula: Adjusted plasma volume = ideal body weight × 0.044 + excess weight × 0.010 (61).

To facilitate workflow, we evaluated the importance of early and late time points that do not affect ascertainment of the critical parts of the enrichment curve (the rise to peak enrichment and the descending slope). Time points 0.5, 1.5, 70, and 94 hours were later omitted from laboratory separation after determining they did not affect fitted curves or the FCRs.

Pool sizes of plasma total apoA-I were calculated by summing the pool sizes of the E^+ and E^- subspecies. Tracer enrichments of plasma total apoA-I at each time point were constructed by summing the enrichments of apoA-I in the E^+ and E^- subspecies, weighting them by relative pool size. Pool sizes of apoA-I in the $CIII^-$ and $CIII^+$ subspecies were determined by summing the pool sizes in the relevant subspecies: E^-CIII^- and E^+CIII^- to make $CIII^-$ and E^-CIII^+ and E^+CIII^+ to make $CIII^+$. Tracer enrichments of apoA-I in the $CIII^-$ and $CIII^+$ subspecies were constructed by summing the enrichments of apoA-I in the relevant subfractions (see above) and weighting them by relative pool size. These methods are summarized in Figure 1.

Model development and kinetic analysis. Compartmental modeling was performed using SAAM-II (The Epsilon Group, Charlottesville, Virginia, USA) (43). We constructed models using prior knowledge about human HDL physiology (41). The input is a forcing function using free plasma leucine isotopic enrichment. The model outputs were rate constants (in pools/hour, converted to pools/day) and flux measurements (in mg/hour, converted to mg/day), each with a standard deviation and 95% CI. For each HDL subspecies, we chose the most parsimonious model that had the most favorable statistics. FCRs for a specific HDL subspecies were calculated by summing all the rate constants out of the compartment for that subspecies. All models were initially established by using the average data of the subjects, and then the data for each subject were modeled individually. For a full description of the modeling process, please see the Supplemental Methods.

Plasma lipid and apolipoprotein measurements. Plasma concentrations of lipids and apolipoproteins were measured at time zero of the infusion protocol. Total plasma cholesterol and triglycerides were measured using an enzymatic assay (Thermo Fisher Scientific). HDL-C was measured as above in the supernatant of plasma after the precipitation of apoB-containing lipoproteins with dextran sulfate (50,000 MW, Genzyme). LDL-C was estimated using the Friedewald equation (62). ELISA using affinity-purified antibodies (Academy Bio-Medical Co.) was performed to measure plasma concentrations of apoA-I, apoE, apoCIII, and apoB. HDL subspecies according to apoCIII were measured in plasma samples stored at –80°C. A sandwich ELISA approach was applied as previously described (63). ELISA plates were read with a BioTek Synergy HT 96-well plate reader controlled by Gen5 1.10 software. All assays were completed in triplicate, and any sample with an intraassay coefficient of variation > 15% was repeated. Final data were exported to Microsoft Excel for analysis and database management.

Molar ratios. HDL subspecies were generated using immunoaffinity column chromatography as described above. Cholesterol content of each subspecies was measured using a commercially available enzymatic assay as described above. The concentrations of apoA-I, apoE, and apoCIII on each HDL subspecies were determined by sandwich ELISA (9). The molar ratios of apoE/apoA-I and apoCIII/apoA-I were calculated using the molecular weights of the 3 apolipoproteins. Cholesterol ratios were determined by dividing the cholesterol content of each subspecies by the plasma apoA-I concentration.

ApoE genotyping. We performed genotyping on buffy coat samples using the ABI PRISM 7900HT Sequence Detection System (Applied Biosystems), in 384-well format. The 5′ nuclease assay (TaqMan) was used to distinguish the 2 alleles of a gene. PCR amplification was carried out on 5–20 ng DNA using 1× TaqMan universal PCR master mix (No Amperase UNG) in a 5 ml reaction volume. Amplification conditions on an AB 9700 dual plate thermal cycler (Applied Biosystems) were as follows: 1 cycle of 95°C for 10 minutes, followed by 50 cycles of 92°C for 15 seconds and 60°C for 1 minute. TaqMan assays were ordered using the ABI Assays-on-Demand service.

CHD assessment. Information on CHD (nonfatal MI and fatal CHD) during follow-up until 2008 was obtained as previously described (64). Briefly, the unique personal identification number assigned to all Danish citizens in the Danish Civil Registration System allowed identification of hospital discharges in the Danish National Register of Patients and the Cause of Death Register. Registers provided information on first-time discharge diagnosis of MI (International Classification of Diseases [ICD], 8th revision codes 410–410.99; and ICD 10th revision codes I21.0–I21.9) and diagnosis of sudden cardiac death diagnosis (ICD 8: 427.27 or ICD 10: I46.0-I46.9) if the cardiac arrest after validation was believed to be caused by an MI. The diagnosis of registered MIs was verified with hospital medical records (65), which were reviewed in accordance with current guidelines (66). This registry has a high degree of validity in recorded MIs (65).

Data accessibility. The authors declare that all data relevant to supporting the conclusions of this study are present within the manuscript and its Supplemental Methods.

Statistics. The results are presented as means ± SEM unless otherwise specified. Paired 2-tailed *t* tests were used to compare 2 parameters in the same participants (for example, apoA-I pool sizes, FCRs, and fluxes in HDL containing or not containing apoE). Overall differences in FCRs, fluxes, and pool sizes across the 4 HDL subspecies were examined using a mixed effects model with HDL subspecies as a fixed factor and participant ID as a random factor. Tests to compare HDL subspecies were carried out independently in each HDL size. Significance was denoted as $P < 0.05$ unless otherwise specified. All statistical analysis was performed using Stata 14 or GraphPad Prism 7. This study had greater than 90% power to detect significant ($P < 0.05$) differences in FCR between apoE-containing and nonapoE-containing subspecies.

We evaluated the baseline characteristics of participants with incident CHD during the follow-up period and the random subcohort separately. Wilcoxon rank-sum tests and χ^2 tests were performed to compare continuous and categorical characteristics of cases and controls.

Spearman correlation coefficients were used to evaluate the association of apoE in HDL containing or not containing apoCIII with HDL, apoCIII, HDL containing or not containing apoCIII, apoB, and triglycerides. We estimated HRs and 95% CI for CHD using Cox proportional hazards regression with standard inverse probability weights and age used as the underlying time scale and stratification by sex. To account for oversampling of cases, female noncases were given a weight of 24,658/917 and male noncases were given a weight of 28,785/842, corresponding to the number of men or women in the full cohort (sex-specific counts of noncases in the overall cohort divided by the sex-specific counts of noncases in the random subcohort). We assessed the proportionality of hazards over time (age) by including an interaction term of the HDL subspecies with age as a covariate. Apolipoprotein measures were modeled continuous ($\log_2$-transformed) and as quintiles based on the distribution of the subcohort. Wald tests for trend were performed with apolipoprotein variables modeled as the median of each quintile. We first adjusted for laboratory batch, smoking status (never; former; current <15, 15–24, ≥25 g/day), education (missing, <8; 8–10; >10 years), alcohol intake (nondrinker; drinker <5, 5–9, 10–19, 20–39, ≥40 g/alcohol/day), BMI (<25; 25–<30; >30 kg/m^2), self-reported diagnosis of hypertension, and self-reported diagnosis of diabetes at baseline. In subsequent models, we additionally adjusted for HDL, apoCIII, triglycerides, and apoB. Models included apoE in HDL containing apoCIII and HDL not containing apoCIII simultaneously, and likelihood ratio tests were used to assess slope heterogeneity of the 2 HDL subspecies containing or not containing apoCIII with the null hypothesis of them being equal. All analyses were performed using STATA 12.1 statistical software (StataCorp).

Study approval. The study was performed in accordance with the principles of the Declaration of Helsinki, and all participants gave written informed consent. Procedures of the metabolic study were approved by the Human Subjects Committees at Brigham and Women's Hospital. The Danish DCH study was approved by the National Committee on Health Research Ethics and the Danish Data Protection Agency (KF 01-116/96).

Author contributions

AMM performed all of the laboratory experiments with help from LW and developed the kinetic models. MK analyzed the case-cohort study data. AMM and MK interpreted all results and wrote the manuscript. COM and JDF conceived and designed experiments. AT and KO had oversight of the Danish DCH study. FMS and MKJ secured funding, conceived and designed experiments, interpreted all results, and edited the manuscript. All authors discussed the results and provided input on the manuscript.

Acknowledgments

The authors would like to acknowledge Louise Bishop and the dietetics team at the CTSC at Brigham and Women's Hospital for their assistance with participant recruitment and the dietary protocol. The authors would also like to acknowledge Jane Lee, Warren Fletcher, Barry Guglielmo, Meghan Bettencourt, and Sue Wong-Lee for technical assistance and Vanessa Byles for assistance with apoE genotyping. We thank all participants of the DCH study for their invaluable contribution to the study. This work was supported by NIH grant R01HL095964 to FMS and by a grant to the Harvard CTSC (8UL1TR0001750) from the National Center for Advancing Translational Science. The DCH study is supported by the Danish Research Council and the Danish Cancer Society. HDL apoCIII measurements were funded by a Young Elite Research Award from the Danish Council of Independent Research, Ministry of Higher Education & Science. Manja Koch is recipient of a Postdoctoral Research Fellowship from the German Research Foundation (Deutsche Forschungsgemeinschaft, KO 5187/1-1). The funding sources had no role in the design and conduct of the study.

Address correspondence to: Frank M. Sacks, 665 Huntington Avenue, Boston, Massachusetts 02115, USA. Phone: 617.432.1420; Email: fsacks@hsph.harvard.edu.

1. Writing Group Members, et al. Heart Disease and Stroke Statistics-2016 Update: A Report From the American Heart Association. *Circulation*. 2016;133(4):e38–360.
2. Gordon T, Castelli WP, Hjortland MC, Kannel WB, Dawber TR. High density lipoprotein as a protective factor against coronary heart disease. The Framingham Study. *Am J Med*. 1977;62(5):707–714.
3. Thompson A, Danesh J. Associations between apolipoprotein B, apolipoprotein AI, the apolipoprotein B/AI ratio and coronary heart disease: a literature-based meta-analysis of prospective studies. *J Intern Med*. 2006;259(5):481–492.
4. Barter PJ, et al. Effects of torcetrapib in patients at high risk for coronary events. *N Engl J Med*. 2007;357(21):2109–2122.
5. Schwartz GG, et al. Effects of dalcetrapib in patients with a recent acute coronary syndrome. *N Engl J Med*. 2012;367(22):2089–2099.
6. AIM-HIGH Investigators, et al. Niacin in patients with low HDL cholesterol levels receiving intensive statin therapy. *N Engl J Med*. 2011;365(24):2255–2267.
7. Lincoff AM, et al. Evacetrapib and Cardiovascular Outcomes in High-Risk Vascular Disease. *N Engl J Med*. 2017;376(20):1933–1942.
8. Gordon SM, Deng J, Lu LJ, Davidson WS. Proteomic characterization of human plasma high density lipoprotein fractionated by gel filtration chromatography. *J Proteome Res*. 2010;9(10):5239–5249.
9. Talayero B, Wang L, Furtado J, Carey VJ, Bray GA, Sacks FM. Obesity favors apolipoprotein E- and C-III-containing high density lipoprotein subfractions associated with risk of heart disease. *J Lipid Res*. 2014;55(10):2167–2177.
10. Mahley RW, Innerarity TL. Lipoprotein receptors and cholesterol homeostasis. *Biochim Biophys Acta*. 1983;737(2):197–222.
11. Beisiegel U, Weber W, Ihrke G, Herz J, Stanley KK. The LDL-receptor-related protein, LRP, is an apolipoprotein E-binding protein. *Nature*. 1989;341(6238):162–164.
12. Mahley RW, Weisgraber KH, Innerarity TL. Interaction of plasma lipoproteins containing apolipoproteins B and E with heparin and cell surface receptors. *Biochim Biophys Acta*. 1979;575(1):81–91.
13. Futamura M, Dhanasekaran P, Handa T, Phillips MC, Lund-Katz S, Saito H. Two-step mechanism of binding of apolipoprotein E to heparin: implications for the kinetics of apolipoprotein E-heparan sulfate proteoglycan complex formation on cell surfaces. *J Biol Chem*. 2005;280(7):5414–5422.
14. Williams KJ, Chen K. Recent insights into factors affecting remnant lipoprotein uptake. *Curr Opin Lipidol*. 2010;21(3):218–228.
15. Gonzales JC, Gordts PL, Foley EM, Esko JD. Apolipoproteins E and AV mediate lipoprotein clearance by hepatic proteoglycans. *J Clin Invest*. 2013;123(6):2742–2751.
16. Tomiyasu K, Walsh BW, Ikewaki K, Judge H, Sacks FM. Differential metabolism of human VLDL according to content of ApoE and ApoC-III. *Arterioscler Thromb Vasc Biol*. 2001;21(9):1494–1500.
17. Zheng C, Khoo C, Ikewaki K, Sacks FM. Rapid turnover of apolipoprotein C-III-containing triglyceride-rich lipoproteins contributing to the formation of LDL subfractions. *J Lipid Res*. 2007;48(5):1190–1203.
18. Mahley RW, Huang Y, Weisgraber KH. Putting cholesterol in its place: apoE and reverse cholesterol transport. *J Clin Invest*. 2006;116(5):1226–1229.
19. Koo C, Innerarity TL, Mahley RW. Obligatory role of cholesterol and apolipoprotein E in the formation of large cholesterol-enriched and receptor-active high density lipoproteins. *J Biol Chem*. 1985;260(22):11934–11943.
20. Settasatian N, Barter PJ, Rye KA. Remodeling of apolipoprotein E-containing spherical reconstituted high density lipoproteins by phospholipid transfer protein. *J Lipid Res*. 2008;49(1):115–126.
21. Peters-Libeu CA, Newhouse Y, Hatters DM, Weisgraber KH. Model of biologically active apolipoprotein E bound to dipalmitoylphosphatidylcholine. *J Biol Chem*. 2006;281(2):1073–1079.
22. Kypreos KE, Zannis VI. Pathway of biogenesis of apolipoprotein E-containing HDL in vivo with the participation of ABCA1 and LCAT. *Biochem J*. 2007;403(2):359–367.
23. Innerarity TL, Pitas RE, Mahley RW. Receptor binding of cholesterol-induced high-density lipoproteins containing predominantly apoprotein E to cultured fibroblasts with mutations at the low-density lipoprotein receptor locus. *Biochemistry*. 1980;19(18):4359–4365.
24. Hui DY, Innerarity TL, Mahley RW. Lipoprotein binding to canine hepatic membranes. Metabolically distinct apo-E and apo-

B,E receptors. *J Biol Chem*. 1981;256(11):5646–5655.
25. Funke H, Boyles J, Weisgraber KH, Ludwig EH, Hui DY, Mahley RW. Uptake of apolipoprotein E-containing high density lipoproteins by hepatic parenchymal cells. *Arteriosclerosis*. 1984;4(5):452–461.
26. Blum CB, Deckelbaum RJ, Witte LD, Tall AR, Cornicelli J. Role of apolipoprotein E-containing lipoproteins in abetalipoproteinemia. *J Clin Invest*. 1982;70(6):1157–1169.
27. Ikewaki K, Rader DJ, Zech LA, Brewer HB. In vivo metabolism of apolipoproteins A-I and E in patients with abetalipoproteinemia: implications for the roles of apolipoproteins B and E in HDL metabolism. *J Lipid Res*. 1994;35(10):1809–1819.
28. Clavey V, Lestavel-Delattre S, Copin C, Bard JM, Fruchart JC. Modulation of lipoprotein B binding to the LDL receptor by exogenous lipids and apolipoproteins CI, CII, CIII, and E. *Arterioscler Thromb Vasc Biol*. 1995;15(7):963–971.
29. Sacks FM. The crucial roles of apolipoproteins E and C-III in apoB lipoprotein metabolism in normolipidemia and hypertriglyceridemia. *Curr Opin Lipidol*. 2015;26(1):56–63.
30. Mendivil CO, Zheng C, Furtado J, Lel J, Sacks FM. Metabolism of very-low-density lipoprotein and low-density lipoprotein containing apolipoprotein C-III and not other small apolipoproteins. *Arterioscler Thromb Vasc Biol*. 2010;30(2):239–245.
31. Watts GF, et al. Differential regulation of lipoprotein kinetics by atorvastatin and fenofibrate in subjects with the metabolic syndrome. *Diabetes*. 2003;52(3):803–811.
32. Sehayek E, Eisenberg S. Mechanisms of inhibition by apolipoprotein C of apolipoprotein E-dependent cellular metabolism of human triglyceride-rich lipoproteins through the low density lipoprotein receptor pathway. *J Biol Chem*. 1991;266(27):18259–18267.
33. Shelburne F, Hanks J, Meyers W, Quarfordt S. Effect of apoproteins on hepatic uptake of triglyceride emulsions in the rat. *J Clin Invest*. 1980;65(3):652–658.
34. de Silva HV, et al. Overexpression of human apolipoprotein C-III in transgenic mice results in an accumulation of apolipoprotein B48 remnants that is corrected by excess apolipoprotein E. *J Biol Chem*. 1994;269(3):2324–2335.
35. Aalto-Setälä K, Weinstock PH, Bisgaier CL, Wu L, Smith JD, Breslow JL. Further characterization of the metabolic properties of triglyceride-rich lipoproteins from human and mouse apoC-III transgenic mice. *J Lipid Res*. 1996;37(8):1802–1811.
36. Zheng C, Khoo C, Furtado J, Sacks FM. Apolipoprotein C-III and the metabolic basis for hypertriglyceridemia and the dense low-density lipoprotein phenotype. *Circulation*. 2010;121(15):1722–1734.
37. Vaisar T, et al. Shotgun proteomics implicates protease inhibition and complement activation in the antiinflammatory properties of HDL. *J Clin Invest*. 2007;117(3):746–756.
38. Sacks FM, et al. VLDL, apolipoproteins B, CIII, and E, and risk of recurrent coronary events in the Cholesterol and Recurrent Events (CARE) trial. *Circulation*. 2000;102(16):1886–1892.
39. Wilson HM, Patel JC, Russell D, Skinner ER. Alterations in the concentration of an apolipoprotein E-containing subfraction of plasma high density lipoprotein in coronary heart disease. *Clin Chim Acta*. 1993;220(2):175–187.
40. Jensen MK, et al. HDL Subspecies Defined by Presence of Apolipoprotein C-III and Incident Coronary Heart Disease in Four Cohorts [published online ahead of print November 21, 2017]. *Circulation*. https://doi.org/10.1161/CIRCULATIONAHA.117.031276.
41. Mendivil CO, Furtado J, Morton AM, Wang L, Sacks FM. Novel Pathways of Apolipoprotein A-I Metabolism in High-Density Lipoprotein of Different Sizes in Humans. *Arterioscler Thromb Vasc Biol*. 2016;36(1):156–165.
42. Rosenson RS, et al. HDL measures, particle heterogeneity, proposed nomenclature, and relation to atherosclerotic cardiovascular events. *Clin Chem*. 2011;57(3):392–410.
43. Barrett PH, et al. SAAM II: Simulation, Analysis, and Modeling Software for tracer and pharmacokinetic studies. *Metab Clin Exp*. 1998;47(4):484–492.
44. Innerarity TL, Pitas RE, Mahley RW. Binding of arginine-rich (E) apoprotein after recombination with phospholipid vesicles to the low density lipoprotein receptors of fibroblasts. *J Biol Chem*. 1979;254(10):4186–4190.
45. Vedhachalam C, et al. The C-terminal lipid-binding domain of apolipoprotein E is a highly efficient mediator of ABCA1-dependent cholesterol efflux that promotes the assembly of high-density lipoproteins. *Biochemistry*. 2007;46(10):2583–2593.
46. Zannis VI, et al. Discrete roles of apoA-I and apoE in the biogenesis of HDL species: lessons learned from gene transfer studies in different mouse models. *Ann Med*. 2008;40 Suppl 1:14–28.
47. Hafiane A, Bielicki JK, Johansson JO, Genest J. Apolipoprotein E derived HDL mimetic peptide ATI-5261 promotes nascent HDL formation and reverse cholesterol transport in vitro. *Biochim Biophys Acta*. 2014;1842(10):1498–1512.
48. Patsch JR, Gotto AM, Olivercrona T, Eisenberg S. Formation of high density lipoprotein2-like particles during lipolysis of very low density lipoproteins in vitro. *Proc Natl Acad Sci USA*. 1978;75(9):4519–4523.
49. Cheung MC, Sibley SD, Palmer JP, Oram JF, Brunzell JD. Lipoprotein lipase and hepatic lipase: their relationship with HDL subspecies Lp(A-I) and Lp(A-I,A-II). *J Lipid Res*. 2003;44(8):1552–1558.
50. Davidson WS, Silva RA. Apolipoprotein structural organization in high density lipoproteins: belts, bundles, hinges and hairpins. *Curr Opin Lipidol*. 2005;16(3):295–300.
51. Matsuura F, Wang N, Chen W, Jiang XC, Tall AR. HDL from CETP-deficient subjects shows enhanced ability to promote cholesterol efflux from macrophages in an apoE- and ABCG1-dependent pathway. *J Clin Invest*. 2006;116(5):1435–1442.
52. Mahley RW. Apolipoprotein E: cholesterol transport protein with expanding role in cell biology. *Science*. 1988;240(4852):622–630.
53. Singh SA, et al. Multiple apolipoprotein kinetics measured in human HDL by high-resolution/accurate mass parallel reaction monitoring. *J Lipid Res*. 2016;57(4):714–728.
54. Hime NJ, Drew KJ, Hahn C, Barter PJ, Rye KA. Apolipoprotein E enhances hepatic lipase-mediated hydrolysis of reconstituted high-density lipoprotein phospholipid and triacylglycerol in an isoform-dependent manner. *Biochemistry*. 2004;43(38):12306–12314.
55. Jensen MK, Rimm EB, Furtado JD, Sacks FM. Apolipoprotein C-III as a Potential Modulator of the Association Between HDL-Cholesterol and Incident Coronary Heart Disease. *J Am Heart Assoc*. 2012;1(2):jah3-e000232.
56. Riwanto M, et al. Altered activation of endothelial anti- and proapoptotic pathways by high-density lipoprotein from patients with coronary artery disease: role of high-density lipoprotein-proteome remodeling. *Circulation*. 2013;127(8):891–904.
57. Chivot L, et al. Logistic discriminant analysis of lipids and apolipoproteins in a population of coronary bypass patients and the significance of apolipoproteins C-III and E. *Atherosclerosis*. 1990;82(3):205–211.
58. Prentice RL. A case-cohort design for epidemiologic cohort studies and disease prevention trials. *Biometrika*. 1986;73(1):1–11.

59. Kim RS. A new comparison of nested case-control and case-cohort designs and methods. *Eur J Epidemiol*. 2015;30(3):197–207.
60. Tjønneland A, et al. Study design, exposure variables, and socioeconomic determinants of participation in Diet, Cancer and Health: a population-based prospective cohort study of 57,053 men and women in Denmark. *Scand J Public Health*. 2007;35(4):432–441.
61. Nikkilä EA, Kekki M. Plasma triglyceride metabolism in thyroid disease. *J Clin Invest*. 1972;51(8):2103–2114.
62. Friedewald WT, Levy RI, Fredrickson DS. Estimation of the concentration of low-density lipoprotein cholesterol in plasma, without use of the preparative ultracentrifuge. *Clin Chem*. 1972;18(6):499–502.
63. Mendivil CO, Rimm EB, Furtado J, Chiuve SE, Sacks FM. Low-density lipoproteins containing apolipoprotein C-III and the risk of coronary heart disease. *Circulation*. 2011;124(19):2065–2072.
64. Jensen MK, et al. Obesity, behavioral lifestyle factors, and risk of acute coronary events. *Circulation*. 2008;117(24):3062–3069.
65. Joensen AM, et al. Predictive values of acute coronary syndrome discharge diagnoses differed in the Danish National Patient Registry. *J Clin Epidemiol*. 2009;62(2):188–194.
66. Luepker RV, et al. Case definitions for acute coronary heart disease in epidemiology and clinical research studies: a statement from the AHA Council on Epidemiology and Prevention; AHA Statistics Committee; World Heart Federation Council on Epidemiology and Prevention; the European Society of Cardiology Working Group on Epidemiology and Prevention; Centers for Disease Control and Prevention; and the National Heart, Lung, and Blood Institute. *Circulation*. 2003;108(20):2543–2549.